Development 140, 66-75 (2013) doi:10.1242/dev.084103

Dose-dependent roles for canonical Wnt signalling in *de novo* crypt formation and cell cycle properties of the colonic epithelium

Akihiro Hirata[1,*], Jochen Utikal[2,3,*], Satoshi Yamashita[4], Hitomi Aoki[5], Akira Watanabe[6], Takuya Yamamoto[6], Hideyuki Okano[7], Nabeel Bardeesy[2], Takahiro Kunisada[5], Toshikazu Ushijima[4], Akira Hara[8], Rudolf Jaenisch[9], Konrad Hochedlinger[2,‡] and Yasuhiro Yamada[6,10,‡]

SUMMARY

There is a gradient of β-catenin expression along the colonic crypt axis with the highest levels at the crypt bottom. In addition, colorectal cancers show a heterogeneous subcellular pattern of β-catenin accumulation. However, it remains unclear whether different levels of Wnt signalling exert distinct roles in the colonic epithelium. Here, we investigated the dose-dependent effect of canonical Wnt activation on colonic epithelial differentiation by controlling the expression levels of stabilised β-catenin using a doxycycline-inducible transgenic system in mice. We show that elevated levels of Wnt signalling induce the amplification of Lgr5+ cells, which is accompanied by crypt fission and a reduction in cell proliferation among progenitor cells. By contrast, lower levels of β-catenin induction enhance cell proliferation rates of epithelial progenitors without affecting crypt fission rates. Notably, slow-cycling cells produced by β-catenin activation exhibit activation of Notch signalling. Consistent with the interpretation that the combination of Notch and Wnt signalling maintains crypt cells in a low proliferative state, the treatment of β-catenin-expressing mice with a Notch inhibitor turned such slow-cycling cells into actively proliferating cells. Our results indicate that the activation of the canonical Wnt signalling pathway is sufficient for *de novo* crypt formation, and suggest that different levels of canonical Wnt activations, in cooperation with Notch signalling, establish a hierarchy of slower-cycling stem cells and faster-cycling progenitor cells characteristic for the colonic epithelium.

KEY WORDS: Wnt signalling, Notch signalling, Intestinal stem cell, Mouse

INTRODUCTION

The intestinal epithelium is characterised by rapid and continuous renewal throughout life. One of the major players involved in the renewal of the intestinal epithelium is the canonical Wnt signalling pathway. Experimental manipulation of Wnt signalling has been shown to influence epithelial proliferation in the intestines (Korinek et al., 1998; Pinto et al., 2003; Kuhnert et al., 2004; Sansom et al., 2004; Andreu et al., 2005; Fevr et al., 2007). For example, inactivation of Wnt signalling by transgenic or adenoviral expression of *Dickkopf1* (*Dkk1*), a secreted Wnt inhibitor, leads to marked inhibition of epithelial proliferation in the intestines (Pinto et al., 2003; Kuhnert et al., 2004). By contrast, two independent groups have demonstrated that loss of *Apc* results in a rapid and dramatic enlargement of the crypt compartment associated with abnormal cell proliferation in the small intestine (Sansom et al., 2004; Andreu et al., 2005). Together, these experiments provide definitive evidence for the importance of Wnt signalling in controlling intestinal epithelial proliferation.

In addition to controlling cell proliferation, a role for Wnt/β-catenin signalling in stem cell maintenance in the intestine has been suggested. Inactivation of Wnt signalling by either overexpression of *Dkk1* or conditional deletion of *Ctnnb1* (the gene encoding β-catenin) results in the loss of intestinal crypts, indicating that Wnt signalling is indispensable for stem cell maintenance (Pinto et al., 2003; Kuhnert et al., 2004; Fevr et al., 2007). In fact, the intestinal stem cell (ISC) marker *Lgr5* has initially been identified as a target of β-catenin/Tcf transcription (Barker et al., 2007), which is in accordance with the view that ISCs harbour a higher activity of canonical Wnt signals. In further support of this notion, nuclear accumulation of β-catenin has been observed at the crypt bottom in cells that potentially include ISCs (van de Wetering et al., 2002).

The number of ISCs has to be tightly regulated in the intestinal crypts in order to facilitate tissue turnover but prevent abnormal growth. ISCs are usually involved in a process of homeostatic self-renewal in the adult intestine but can also be rapidly recruited to repair tissues after injury. Indirect evidence for an involvement of Wnt signalling in stem cell amplification derives from a study showing that PTEN deficiency increases the frequency of crypt fission/budding and the number of cells expressing *Musashi1*, a putative ISC marker, through activated Wnt signalling (He et al., 2007). However, the underlying mechanism by which activated Wnt signalling may expand ISCs remains elusive, and direct evidence

[1]Division of Animal Experiment, Life Science Research Center, Gifu University, 1-1 Yanagido, Gifu, 501-1194, Japan. [2]Massachusetts General Hospital Cancer Center and Center for Regenerative Medicine, Harvard Stem Cell Institute, 185 Cambridge Street, Boston, MA 02114, USA. [3]Skin Cancer Unit, German Cancer Research Center, Heidelberg, Germany and Department of Dermatology, Venereology and Allergology, University Medical Center Mannheim, Ruprecht-Karl University of Heidelberg, Mannheim, Germany. [4]Division of Epigenomics, National Cancer Center Research Institute, 5-1-1 Tsukiji, Chuo-ku, Tokyo, Japan. [5]Department of Tissue and Organ Development and [8] Department of Tumor Pathology, Gifu University Graduate School of Medicine, 1-1 Yanagido, Gifu, 501-1194, Japan. [6]Center for iPS Cell Research and Application (CiRA), Institute for Integrated Cell-Material Sciences (WPI-iCeMS), Kyoto University, 53 Kawahara-cho, Shogoin, Sakyo-ku, Kyoto 606-8507, Japan. [7]Department of Physiology, Keio University School of Medicine, 35 Shinanomach, Shinjuku-ku, Tokyo 160-8582, Japan. [9]Whitehead Institute for Biomedical Research, Massachusetts Institute of Technology, Cambridge, MA 02142, USA. [10]PRESTO, Japan Science and Technology Agency, Saitama, Japan.

*These authors contributed equally to this work
‡Authors for correspondence (khochedlinger@helix.mgh.harvard.edu; y-yamada@cira.kyoto-u.ac.jp)

Accepted 15 October 2012

that elevated Wnt signalling is sufficient for stem cell expansion in the adult intestine is lacking.

Disruption of canonical Wnt signalling is involved in the vast majority of colon cancers. Mutation in *APC* or *CTNNB1* is the initiating event in the transformation of colonic epithelial cells, which lead to the constitutive activation of Wnt signalling. Importantly, despite the presence of the activating mutations for Wnt signalling, colorectal cancers show cellular heterogeneity of β-catenin accumulation within a tumour mass. Immunohistochemical studies have revealed that nuclear β-catenin accumulation, the hallmark of activated Wnt signalling, is observed in a subset of colon tumour cells (Brabletz et al., 2001; Jung et al., 2001; Fodde and Brabletz, 2007). Furthermore, a recent study indicates that colon tumour cells with high Wnt signalling activity show the properties of cancer stem cells (Vermeulen et al., 2010), which emphasises the need for further studies on the dose-dependent effect of Wnt signalling on intestinal epithelial cells.

Although a large body of literature has established that activation of the canonical Wnt signalling is the dominant force in the maintenance of intestinal homeostasis, other signalling cascades, such as the Notch, BMP and PI3 cascades, have also been implicated in the control of epithelial cell proliferation and stem cell turnover (Scoville et al., 2008). However, it remains poorly understood how these other signalling cascades integrate with Wnt signalling in the intestinal epithelium to control stem cell turnover and epithelial regeneration. It is assumed that the various signalling cascades act in a hierarchical manner, and regulate each other. A better understanding of how the coordinated activity of these signalling cascades maintains intestinal homeostasis is crucial for dissecting the mechanisms of ISCs as well as for attempts to utilise stem cells in regenerative medicine and to target them in diseases such as cancer.

Using a novel β-catenin-inducible mouse model, we show here that elevated levels of activated β-catenin induces *de novo* crypt formation but reduces epithelial cell proliferation among progenitors. However, combined β-catenin overexpression and Notch inhibition turns these slow-cycling cells into proliferating cells. These results imply that β-catenin signalling fulfils dual roles in the control of intestinal epithelial regeneration by (1) promoting crypt formation and (2) activating cell proliferation in cooperation with Notch signalling.

MATERIALS AND METHODS

Mice

Transgenic mice expressing histone H2B-green fluorescent protein (H2B-GFP) fusion protein under the control of a TRE were obtained from Jackson Laboratories [Bar Harbor, ME, USA; strain name: Tg(tetO-HIST1H2BJ/GFP)47Efu] and crossed with mice harbouring a ROSA26 promoter-driven M2rtTA allele (Beard et al., 2006). β-Catenin embryonic stem (ES) cell line was generated with stabilised β-catenin (S33 mutation) cDNA (Morin et al., 1977; van Noort et al., 2002) with use of KH2 ES cell line and injected into blastocysts to produce transgenic mice. Mice of 4 to 8 weeks of age were fed 0.1 or 2.0 mg/ml doxycycline in the drinking water supplemented with 10 mg/ml sucrose. *Lgr5-GFP* knock-in mouse were obtained from Jackson Laboratories (strain name: B6.129P2-*Lgr5*$^{tm1(cre/ESR1)Cle}$/J).

Crypt isolation

Crypts were isolated form the whole colon and caecum by incubation in Hanks' balanced salt solution containing 30 mM EDTA as described previously (Tsukamoto et al., 2001).

Flow cytometry

Isolated crypts were incubated in 1% collagenase type 1 for 15 minutes at 37°C and then 0.25% trypsin/1m M EDTA for 5 minutes at 37°C. Single-cell suspensions were obtained by transfer through nylon mesh to remove large clumps, washing, and resuspension in staining medium containing 0.5 μl/ml propidium iodide (Calbiochem-Novabiochem Corp., San Diego, CA, USA) to eliminate dead cells. The cells were sorted by fluorescence-activated cell sorting (FACS) using a Vantage SE flow cytometer (Becton Dickinson, San Jose, CA, USA).

Microarray analysis

Total RNA was extracted from isolated crypts or FACS-sorted cells as previously reported (Yamashita et al., 2003). Oligonucleotide microarray hybridisation and scanning using GeneChip Mouse Genome 430 2.0 Array (Affimetrix) were performed as previously reported (Yamashita et al., 2003). For the pathway analysis, 907 probe sets, which are specifically upregulated in β-catenin induced cells, but not in H2B-low fast-cycling cells, were selected. The gene enrichment analysis was performed with DAVID PANTHER annotation tool. Microarray data have been deposited in Gene Expression Omnibus database under accession number GSE41688.

Quantitative real-time RT-PCR

qRT-PCR was performed as described previously (Oyama et al., 2008). The expression level of each gene was normalised to the β-actin expression level using the standard curve method. Each experiment was done in either duplicate or triplicate, and then, the average was calculated. Primer sequences for qPCR were taken from PrimerBank. The primer sequences are listed in supplementary material Table S2.

Histological and immunohistochemical analysis

Normal and tumour tissue samples were fixed in 10% buffered formalin, proceeded by standard method and embedded in paraffin. Sections were stained with Haematoxylin and Eosin (H&E), and serial sections were used for immunohistochemical analysis. Immunostaining was performed as described previously (Oyama et al., 2008) using the following antibodies: anti-β-catenin (1:1000 dilution; BD Transduction Laboratories, San Diego, CA, USA), anti-Musashi-1 [1:500 dilution (Kaneko et al., 2000)], anti-BrdU (1:250 dilution; Abcam, Cambridge, UK), anti-Hes1 [1:100 dilution; a gift from Dr Sudo (Ito et al., 2000)], anti-GFP (1:1500 dilution; Invitrogen, Carlsbad, CA, USA), anti-Ki67 (1:250 dilution; Dako Corp., Carpinteria, CA, USA) and anti-chromogranin A (1:1500 dilution; Abcam). Photomicrographs show the distal part of the colon or caecum in the figures.

Bromodeoxyuridine (BrdU) assay

Mice were injected with BrdU intraperitoneally (i.p.) at a dose of 100 mg/kg body weight. Mice were sacrificed 2 or 48 hours after injection, and incorporated BrdU was detected by immunostaining with anti-BrdU antibody as described above.

Notch inhibitor

γ-Secretase inhibitor (MRK003-ONC) was kindly provided by Merck and administrated orally at 100 mg/kg 2 days before sacrifice.

RESULTS

Canonical Wnt signalling is physiologically active in proliferative compartment of colonic crypts

Previous studies have shown by experimental manipulation of the Wnt signalling cascade that canonical Wnt signalling regulates intestinal epithelial proliferation (Korinek et al., 1998; Pinto et al., 2003; Kuhnert et al., 2004; Sansom et al., 2004; Andreu et al., 2005; Fevr et al., 2007). However, whether canonical Wnt signalling is active in the proliferative compartment of normal colonic crypts remains unclear. To address this question, we separated actively proliferating progenitor cells (transit-amplifying cells) from non-proliferating cells in the colon by using transgenic mice that express a histone H2B-GFP fusion protein under the control of a tetracycline-responsive regulatory element (TRE) (Tumbar et al., 2004). H2B-GFP becomes incorporated or diluted in a cell cycle-dependent manner and thus facilitates the separation of frequently dividing cells from infrequently dividing cells in any given tissue,

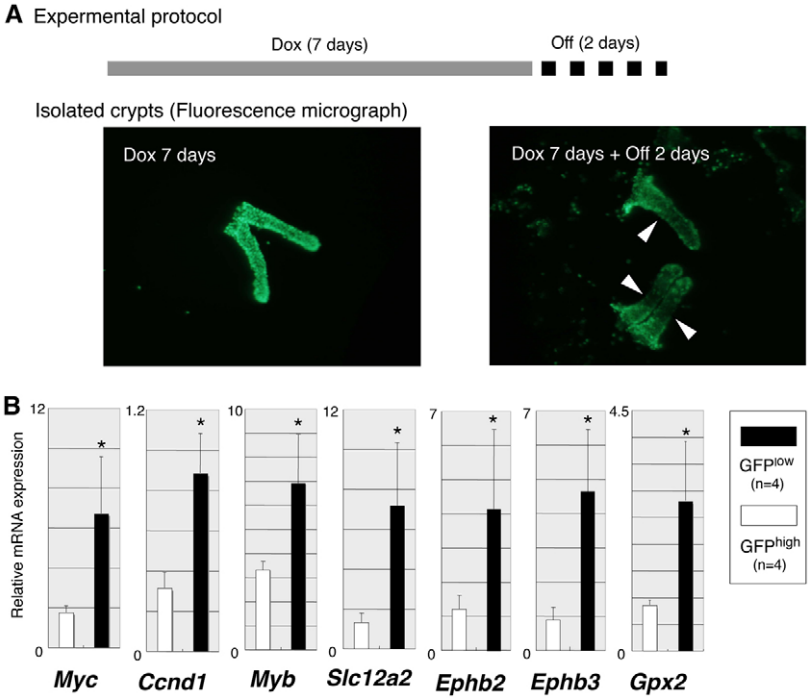

Fig. 1. Upregulation of canonical Wnt target genes in the proliferative compartments of colonic crypts. (**A**) Separation of proliferating cells from non-proliferative cells in the colon of histone H2B-GFP inducible mice. All crypt cells were labelled with nuclear GFP after Histone-GFP induction for 7 days, whereas the subsequent withdrawal of the induction resulted in dilution of the nuclear GFP signals in proliferating progenitor cells according to the cell divisions. Arrowheads indicate the decreased signal of the nuclear GFP at the proliferating compartments. (**B**) qRT-PCR for canonical Wnt target genes in GFP^{low} and GFP^{high} cells. After FACS sorting, the expression of canonical Wnt target genes was analysed by qRT-PCR. Expressions of *Myc*, *Ccnd1*, *Myb*, *Slc12a2*, *Ephb2*, *Ephb3* and *Gpx2* are significantly higher in GFP^{low} cells than in GFP^{high} cells. Data are mean ± s.d.; **P*<0.05, by Mann–Whitney *U*-test.

as has been successfully shown for the skin and haematopoietic system (Tumbar et al., 2004; Foudi et al., 2009). Specifically, H2B-GFP mice were crossed with mice harbouring a *Rosa26* promoter-driven M2 reverse tetracycline transactivator (M2rtTA) allele (Beard et al., 2006) to enable H2B expression in essentially all tissues. In the absence of doxycycline treatment, colonic epithelial cells exhibited no detectable GFP signals, thus excluding leaky expression of the transgene. By contrast, 7 days after doxycycline administration, all crypt cells exhibited a strong nuclear GFP signal (Fig. 1A). When doxycycline was withdrawn for 2 days after the initial labelling period, nuclear GFP signal was diluted in proliferating cells, consistent with rapid cell divisions of progenitor cells, whereas non-proliferating cells retained GFP (Fig. 1A). GFP^{high} non-proliferating and GFP^{low} proliferating epithelial cells were then sorted from the isolated crypts by FACS for subsequent molecular analyses (supplementary material Fig. S1A). To validate our approach to separate proliferating cells from non-proliferating cells using H2B-GFP dilution, we examined the expression levels of cell proliferation-related genes by microarray analysis. As expected, the expression of cyclins and Cdks, including *Ccna2*, *Ccnb1*, *Ccnd1*, *Ccnd2*, *Cdk2*, *Cdk4* and *Cdk6*, was higher in GFP^{low} cells than in GFP^{high} cells, whereas Cdk inhibitors, such as *Cdkn1a* and *Cdkn2b*, were found to be downregulated in GFP^{low} cells compared with GFP^{high} cells. Gene expression of candidates was validated by quantitative RT-PCR (supplementary material Fig. S1B). We also confirmed that GFP^{low} cells contained a higher number of Ki-67 (Mki67 – Mouse Genome Informatics)-positive cells than GFP^{high} cells by immunostaining colon sections of H2B-GFP mouse (supplementary material Fig. S1C). Importantly, we found that a number of canonical Wnt signalling target genes were upregulated in GFP^{low} proliferating cells compared with GFP^{high} non-proliferating cells using microarray analysis. qRT-PCR confirmed a significant upregulation of Wnt target genes (van de Wetering et al., 2002) (Fig. 1B), implying that canonical Wnt signalling is associated with active proliferation of progenitor cells in normal colonic crypts.

Forced induction of β-catenin leads to rapid *de novo* crypt formation in the colon

To investigate the effects of acute Wnt activation on adult intestinal homeostasis, we generated doxycycline-inducible β-catenin mice. This was achieved by targeting a constitutive active version of β-catenin (S33 mutation) under the control of a tetOP minimal promoter into the *Col1a1* locus in ES cells, which were subsequently injected into blastocysts to produce transgenic mice. Unless noted, homozygous transgenic mice were used in the experiment. When we fed adult mice doxycycline in the drinking water (2.0 mg/ml), β-catenin-induced animals became morbid after only 6-8 days. In the colon, 5 days of doxycycline treatment led to nuclear accumulation of β-catenin in the epithelium (Fig. 2A) and strong upregulation of canonical Wnt target genes such as *Myc* and *Ccnd1* (Fig. 2B). Notably, we frequently observed crypt fission and/or branching in β-catenin-induced colon sections, suggesting that the *de novo* crypt formation was induced by β-catenin induction (Fig. 2A). Immunohistological analyses of colon sections from doxycycline-induced chimeric mice demonstrated that the crypt fission/branching phenotype was only seen in β-catenin-induced crypts but not in host embryo-derived crypts, documenting a cell-autonomous effect of β-catenin induction (supplementary material Fig. S2A). We also observed an increase in crypt fission/branching in the crypts of the small intestine (supplementary material Fig. S2B). Analysis of isolated crypts confirmed that the fission and budding of crypts occurred at a significantly higher rate in β-catenin-induced colon than in non-induced colon (Fig. 2C,D). In addition, staining of sections for mucin with Alcian Blue-periodic acid-Schiff (AB-PAS) demonstrated a significant suppression of cellular differentiation towards goblet cells following β-catenin activation (supplementary material Fig. S3A). By contrast, chromogranin A-positive cells were found in both β-catenin-induced and non-induced crypts, showing a lesser effect on the enteroendocrine cell differentiation (supplementary material Fig. S3B). The numbers of chromogranin A-positive cells per crypt were 1.36±1.00 and 1.12±1.10 in β-catenin-induced and non-induced

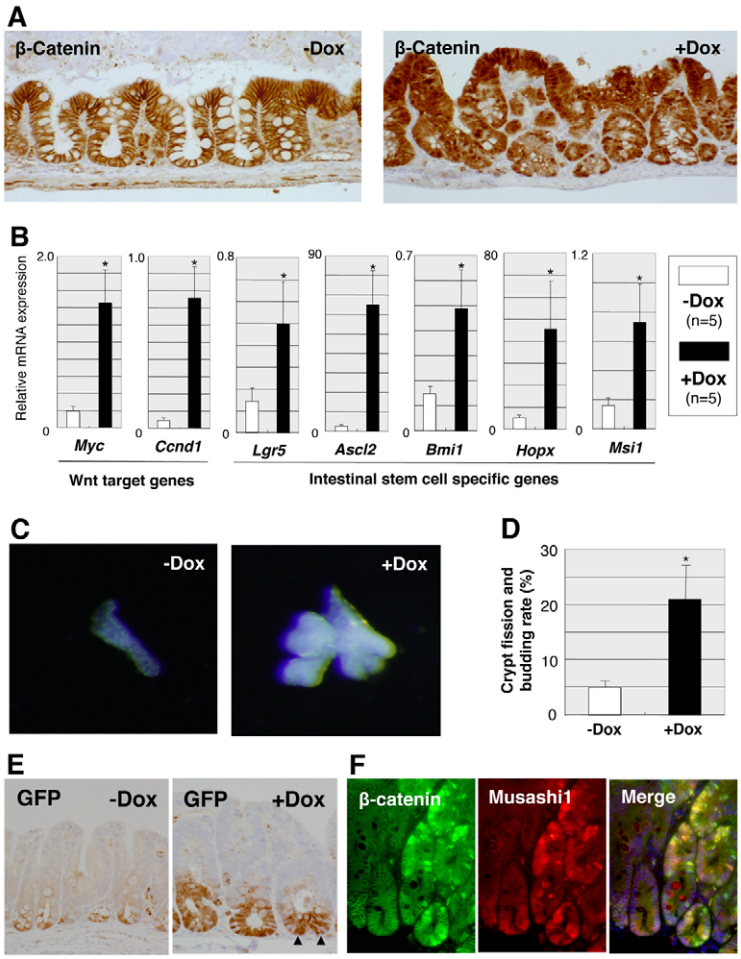

Fig. 2. β-Catenin induction leads to *de novo* crypt formation with increased expression of ISC markers in the colon. (**A**) β-Catenin immunostaining on colonic section of β-catenin-induced mice. Doxycycline treatment results in nuclear accumulation of β-catenin and frequent fission/budding of colonic crypts. (**B**) qRT-PCR for Wnt target genes and ISC-specific genes. The expression of Wnt target genes and ISC-specific genes are significantly upregulated by β-catenin induction. Data are mean ± s.d.; **P*<0.05, by Mann–Whitney *U*-test. (**C**) Isolated colonic crypts from a doxycycline-treated mouse. A drastic crypt budding is observed in the crypt with β-catenin induction. (**D**) Fission/budding rate in isolated crypts from doxycycline-treated mice. Crypt fission/budding occurs at a significantly higher rate in doxycycline-treated mice than in non-treated mice. Data are mean ± s.d.; **P*<0.05, by Mann–Whitney *U*-test. (**E**) Immunostaining for GFP on colonic sections of β-catenin-induced mice with *Lgr5-GFP* knock-in allele. GFP expression reveals an increased number of *Lgr5*-expressing cells at the lower part of colonic crypts in doxycycline-treated mice. Note that GFP-expressing cells are observed at the bottom of a bifurcating crypt (arrowheads). (**F**) Double immunostaining for Musashi1 (red) and β-catenin (green) on a colonic section of a doxycycline-treated chimeric mouse. Musashi1 expression is coincident with increased β-catenin expression.

colonic crypts, respectively, and no statistical significance was found between groups.

Barker et al. demonstrated that in the mouse gastrointestinal tract Lgr5 specifically labels active ISCs, which are located at the crypt base, cycle frequently and replenish the entire epithelium within a week (Barker et al., 2007). Consistent with the fact that *Lgr5* is a target of β-catenin/Tcf transcription (Barker et al., 2007), qRT-PCR demonstrated that β-catenin activation caused a significant increase in *Lgr5* expression (Fig. 2B). To determine whether the number of *Lgr5*-expressing cells has also increased in these mice, we crossed β-catenin-inducible mice with *Lgr5-GFP* knock-in mice, in which the *GFP* gene is regulated by the endogenous *Lgr5* promoter (Barker et al., 2007). Immunohistochemistry for GFP revealed that the number of *Lgr5*-expressing cells had indeed increased by 4.2-fold following β-catenin induction (Fig. 2E; supplementary material Fig. S4). Of note, although nuclear accumulation of β-catenin was observed throughout the crypt epithelium, expanded *Lgr5*-expressing cells were only observed at the lower part of the crypts (Fig. 2E; supplementary material Fig. S4A). This finding suggests that only existing ISCs, and possibly progenitor cells, respond to Wnt activation by producing more *Lgr5*-expressing cells whereas differentiated cells, located at the upper part of the crypts, are unresponsive to forced β-catenin expression. In addition to an increase in *Lgr5* expression, we also observed a strong upregulation of *Ascl2* (Fig. 2B), another active ISC-specific gene (van der Flier et al., 2009). As transgenic expression of *Ascl2* has been recently shown to induce ectopic crypt formation in the intestine (van der Flier et al., 2009), the increased levels of *Ascl2* might explain the observed crypt fission/budding phenotype in β-catenin-induced crypts. In addition to active ISCs, recent reports have indicated that quiescent ISCs are located at position 4 of the small intestine (Li and Clevers, 2010). Interestingly, β-catenin induction increased the expression of markers for the quiescent ISCs as well, including *Bmi1* and *Hopx* (Fig. 2B) (Sangiorgi and Capecchi, 2008; Takeda et al., 2011). Lastly, we examined the expression of Musashi1, a marker for putative stem and early progenitor cells (Potten et al., 2003), and found that β-catenin induction resulted in an upregulation of Musashi1 (Fig. 2B,F) in a cell-autonomous manner (Fig. 2F). Taken together, these data demonstrate that acute activation of β-catenin results in *de novo* crypt formation within a few days in a cell-autonomous fashion, accompanied by the amplification of ISC-like cells.

Colon cells with highest nuclear β-catenin do not actively divide

Previous studies have suggested that the canonical Wnt signalling plays a role in active cell proliferation of the intestine (Sansom et al., 2004; Andreu et al., 2005). In agreement, using the histone H2B-GFP mouse model, we show here that Wnt signalling is active in the proliferating progenitor compartment of normal colonic crypts under physiological conditions (Fig. 1B). To assess directly the effect of Wnt activation on the cell proliferation, we performed double-immunostaining with β-catenin and the proliferation marker Ki-67 on β-catenin-induced colonic sections. Unexpectedly, we found that the majority of cells with nuclear β-catenin failed to stain positively for Ki-67 (Fig. 3A). Instead, Ki-67 staining was

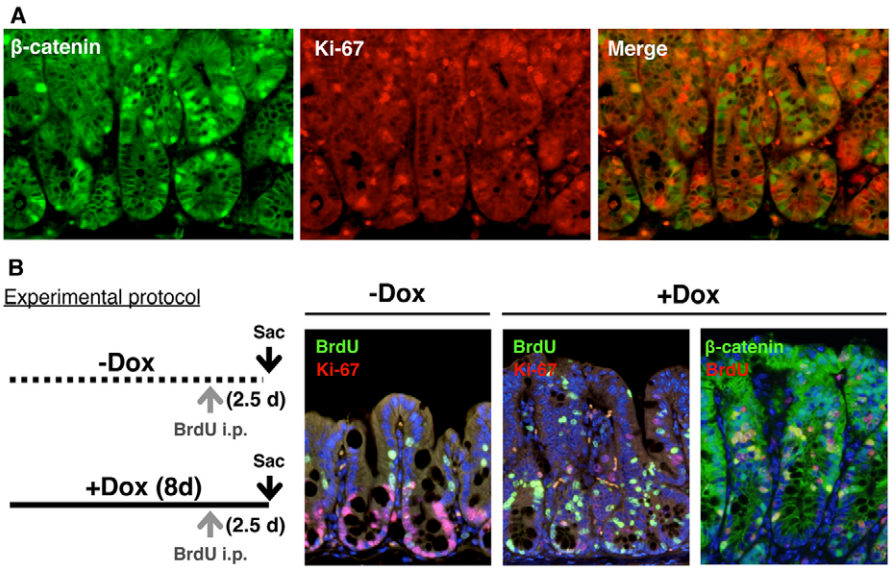

Fig. 3. Slow cycling properties of β-catenin-induced colonic cells. (**A**) Double immunostaining for β-catenin (green) and Ki-67 (red) on a β-catenin-induced colonic section. Majority of colonic cells with strong nuclear β-catenin expression are not coincident with Ki-67. (**B**) A scheme of the BrdU pulse-chase experiment and double immunostaining for Ki-67/BrdU and β-catenin/BrdU. In normal crypts, most proliferating progenitor cells have lost the BrdU retention according to the active cell divisions, and only a small number of cells retain BrdU. By contrast, β-catenin induction leads to an increased number of BrdU-retaining cells. Immunostaining for β-catenin (green) and BrdU (red) shows that BrdU-retaining cells frequently express nuclear β-catenin, indicating that colonic cells with strong nuclear β-catenin divide slowly. Sac, sacrifice.

predominantly observed in cells adjacent to cells with strong nuclear β-catenin signal (Fig. 3A). The majority of Ki-67-positive cells showed cytoplasmic and moderate β-catenin expression (76.7%) on the section, but some Ki-67-positive cells revealed nuclear and strong expression (23.3%). These observations were confirmed by a BrdU incorporation assay. When mice were injected with BrdU (100 mg/kg i.p.) 2 hours before sacrifice, the colonic cells with strong nuclear β-catenin showed less frequent BrdU incorporation (supplementary material Fig. S5A). We infer from this finding that intestinal cells with strong nuclear β-catenin expression did not actively divide. To investigate further the proliferation history of cells after β-catenin induction, we performed a pulse-chase experiment using BrdU (Fig. 3B). Mice were given a single BrdU injection (100 mg/kg i.p.) during the doxycycline treatment and were sacrificed 2 days later (Fig. 3B). β-Catenin induction caused an increased number of BrdU-retaining, i.e. non-dividing, cells near the crypt bottom, whereas non-induced crypts contained a small number of BrdU-retaining cells above the proliferative compartment (Fig. 3B). Furthermore, double-immunostaining for BrdU and β-catenin revealed that BrdU-retaining cells frequently expressed nuclear β-catenin (Fig. 3B). These results imply that, although forced β-catenin activation results in a net increase of cell proliferation in the colon, cells with strong nuclear β-catenin signal divide relatively slowly as measured by Ki-67 proliferation and BrdU label-retention assays. To support these findings, qRT-PCR revealed that the expression of the Cdk inhibitors *Cdkn1a*, *Cdkn1b* and *Cdkn1c* were significantly upregulated in β-catenin-induced colonic crypts (supplementary material Fig. S5B).

β-Catenin overexpression induces activation of Notch

In order to dissect further the molecular mechanisms underlying *de novo* crypt formation upon β-catenin induction, we compared the gene expression profiles of β-catenin-induced and non-induced colon crypts. Briefly, colonic crypts isolated from β-catenin-inducible control mice and from mice fed doxycycline for 5 days were subjected to microarray analysis. Consistent with our finding that β-catenin induction results in *de novo* crypt formation, microarray data confirmed the upregulation of ISC-specific genes, such as *Lgr5*, *Ascl2* and *Hopx*, as well as Wnt target genes in β-catenin-induced colon crypts (supplementary material Table S1). Next, we wished to elucidate the apparent discrepancy between β-catenin-induced *de novo* crypt formation and the observed slow cycling properties of β-catenin-high cells. To this end, we compared gene expression profiles of β-catenin-induced cells and fast-cycling H2B-GFP low cells. Interestingly, pathway analysis revealed that genes in the Notch signalling pathway are specifically upregulated in β-catenin-induced colonic cells compared with fast-cycling normal crypt cells (Fig. 4A). qRT-PCR confirmed that *Hes1*, a well-established target gene of Notch signalling, is strongly induced by β-catenin activation with significant upregulation of Notch ligands (*Jag1* and *Jag2*) and Notch receptors (*Notch1* and *Notch2*) (Fig. 4B). Furthermore, we found that Notch ligands and Notch receptors were significantly upregulated as early as 12 hours after doxycycline treatment (Fig. 5B; see more details below). Consistent with this observation, immunohistochemical analysis revealed the strong nuclear expression of Hes1 on colonic sections of β-catenin-induced mice. (supplementary material Fig. S6). Our results suggest that β-catenin expression might activate Notch signalling through upregulation of its ligands and receptors.

Notch inhibition induces active cell proliferation in slow-cycling cells and blocks crypt fission and budding by β-catenin induction

In order to determine the relative contribution of activated Notch signalling to *de novo* crypt formation and the slow-cycling properties of colonic cells following β-catenin activation, we treated β-catenin-induced mice with a Notch/γ-secretase inhibitor (Fig. 4C). Surprisingly, treatment with a Notch inhibitor induced active proliferation of β-catenin-expressing, slow-cycling cells. Inhibitor-treated crypts were elongated with increased numbers of Ki-67 positive cells (Fig. 4D,E; supplementary material Fig. S7). Importantly, the simple withdrawal of doxycycline treatment (protocol G4) or the administration of Notch inhibitor alone (protocol G5) did not cause abnormal cell proliferation (Fig. 4E), indicating that constitutive Wnt activation is essential for active cell proliferation. To quantify the effect of Notch inhibition on cell proliferation in the presence of β-catenin activation, we performed a pulse-chase experiment with BrdU. Mice were given a single dose of BrdU (100 mg/kg i.p.) during the doxycycline treatment in the presence or absence of Notch inhibitor, and animals were sacrificed 2 days later. Immunohistochemical analysis showed that, in contrast

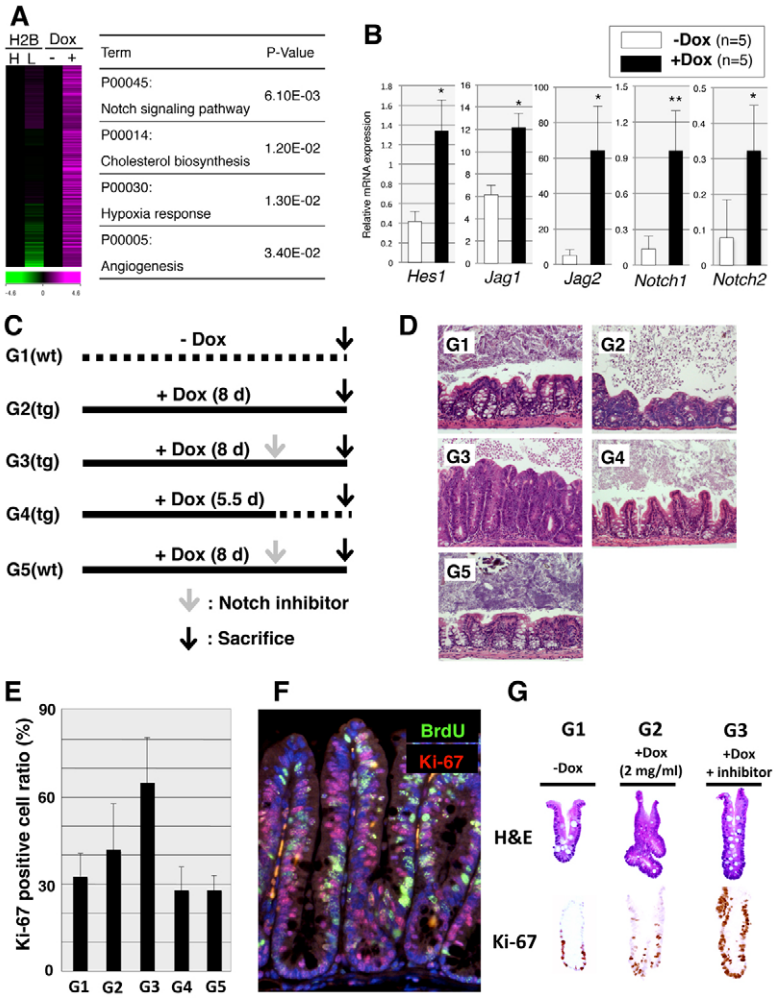

Fig. 4. Notch activation contributes to the maintenance of a slow-cycling state in β-catenin-induced colon. (**A**) Activation of Notch signalling pathway in β-catenin-induced slow-cycling colonic epithelium. Genes specifically upregulated in β-catenin-induced cells, but not in fast-cycling cells (GFP-Low cells in the H2B-GFP experiment) were selected. The heat map shows log2-fold changes in gene expression between β-catenin-induced and non-induced colon (right two columns in the left panel) and between histone-GFP-low and high cells (left two columns). The values for β-catenin non-induced colon and histone-GFP-high cells were used as normalisation for comparison, respectively. Subsequently, gene enrichment analysis were performed using DAVID on the selected genes and revealed that genes in a Notch signalling pathway are significantly concentrated in β-catenin-induced cells. All of the significantly enriched pathways in β-catenin-induced cells are listed in the table. H2B, histone H2B-GFP mouse; H, GFP^{high} cells; L, GFP^{low} cells; Dox, doxycycline treatment for β-catenin induction. (**B**) qRT-PCR analyses of Notch signalling related genes in β-catenin-induce colonic crypts. The Notch target *Hes1*, the Notch ligands *Jag1* and *Jag2*, and the Notch receptors *Notch1* and *Notch2* are strongly upregulated in β-catenin-activated crypts. Data are means ± s.d.; $*P<0.05$, $**P<0.01$, by Mann–Whitney *U*-test. (**C**,**D**) Experimental protocols for treatment with the Notch inhibitor (C) and the representative histology in each group (D). A Notch inhibitor was administrated orally at 2 days prior to sacrifice. (**E**) The Notch inhibitor induces active proliferation in β-catenin-induced colon. Ki-67-positive cell ratio (percentage of Ki-67-positive cells) is significantly higher in G3 than in other groups ($P<0.00001$ for G1, G4 and G5, and $P<0.0005$ for G2, by one-way ANOVA and Turkey's post hoc test, respectively). (**F**) BrdU pulse-chase experiment in mice treated with doxycycline and Notch inhibitor (protocol G3). Double immunostaining for BrdU (green) and Ki-67 (red) on a colon section. The Notch inhibitor reduces BrdU-retention in colonic crypts, whereas it increases Ki-67-positive cells throughout the crypt. (**G**) H&E staining and Ki-67 immunostaining of isolated crypts. The Notch inhibitor induces active cell proliferation and suppressed the *de novo* crypt formation in β-catenin induced crypts.

to the increased number of BrdU-retaining cells following β-catenin induction alone (Fig. 3B), combined treatment with doxycycline and the Notch inhibitor reduced the number of BrdU-retaining nuclei, whereas it increased the number of Ki-67-positive cells (Fig. 4F). These findings suggest that treatment with the Notch inhibitor induces proliferation of slow-cycling cells that have accumulated as a consequence of β-catenin expression. Importantly, treatment of β-catenin-induced mice with the Notch inhibitor also normalised crypt fission and budding rates (Fig. 4G; supplementary material Fig. S8A), which was accompanied by decreased nuclear β-catenin expression without a change in gene expression at the mRNA level (supplementary material Fig. S8B,C). These results indicate that Notch activation contributes to the maintenance of a slow-cycling state and to *de novo* crypt formation in β-catenin-induced colon, and, hence, Notch inhibition turns slow-cycling cells into fast-cycling cells in the context of transgenic β-catenin expression. However, in spite of the clear morphological changes, we could not detect a change in gene expression of the Notch target

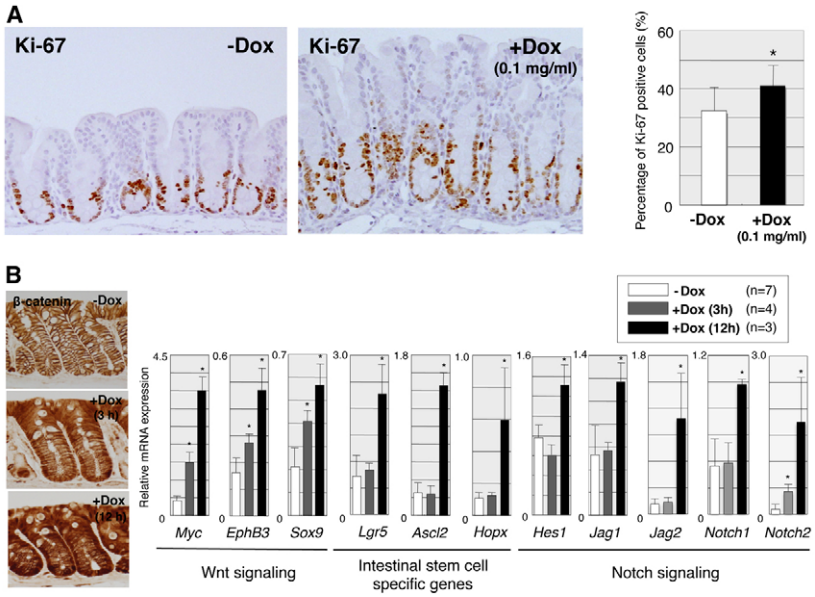

Fig. 5. Dose-dependent effect of Wnt activation on cell proliferation and gene expression in colonic epithelium. (**A**) Lower level of β-catenin induction promotes colonic epithelial proliferation. Ki-67 immunostaining and percentage of Ki-67-positive cells in colonic section from β-catenin-inducible mice treated with lower dose of doxycycline. Lower levels of β-catenin induction increase Ki-67 positive cell ratio and elongate the proliferating compartment of the crypts. Data are mean ± s.d.; **P*<0.05, by Welch's *t*-test. (**B**) Expression of Wnt target genes, ISC-specific genes and Notch signalling-related genes in the colonic crypts with different levels of β-catenin. The different levels of β-catenin accumulation are shown in the left-hand panels. Data are mean ± s.d.; **P*<0.05 compared with non-treated mice, by Kruskal–Wallis test followed by Steel test.

Hes1 in β-catenin-induced mice treated with the Notch inhibitor (data not shown). It is possible that the Notch inhibitor led to a transient inactivation of Notch signalling and thus the altered *Hes1* expression was not detectable at 2 days after treatment. However, given that the Notch/γ-secretase inhibitor has multiple substrates, we cannot completely rule out the possibility that the effect was partly independent of Notch inhibition.

Lower levels of β-catenin activation induce active proliferation of progenitor cells, but not stem cell expansion

In contrast to the well-established role of canonical Wnt signalling in activating cell proliferation in the intestine (Sansom et al., 2004; Andreu et al., 2005), our data show that the Wnt activation confers slow-cycling properties on colonic cells, which is accompanied by *de novo* crypt formation. In an attempt to consolidate these opposing results, we hypothesised that different levels of Wnt signalling may induce different biological outcomes with elevated levels of activation leading to the expansion of slow-cycling ISC-like cells and lower levels of activation inducing active cell proliferation. In order to determine the effects of different levels of β-catenin induction on colon homeostasis, we treated β-catenin-inducible mice with a lower dose of doxycycline than was used previously (0.1 mg/ml in drinking water) and analysed crypt sections. Colonic crypts did not show signs of increased crypt fission/branching rate in mice, suggesting that *de novo* crypt formation is not induced when β-catenin is expressed at low levels (Fig. 5A). However, low levels of β-catenin increased the number of Ki-67-positive cells, and led to an elongation of crypts (Fig. 5A), indicative of enhanced cell proliferation of progenitor cells. These results suggest that different strengths of canonical Wnt signalling result in different transcriptional outputs and, thus, biological effects.

To examine the effects of different levels of Wnt signalling on transcription, we performed gene expression analyses of colonic crypts with high and low levels of β-catenin accumulation. β-Catenin-inducible mice were intragastrically administered doxycycline (100 mg/kg) and sacrificed 3 and 12 hours later, leading to different levels of β-catenin accumulation in the colonic crypts (Fig. 5B). We found that *Myc*, *EphB3* and *Sox9*, well-known targets of canonical Wnt signalling, were upregulated in crypts with both higher and lower levels of β-catenin expression in a level-dependent manner (Fig. 5B). However, activation of the Notch target gene *Hes1* was detected only in crypts with high β-catenin, which is accompanied by the upregulation of ISC-specific genes including *Lgr5*, *Ascl2* and *Hopx* (Fig. 5B). We also examined the gene expression in colonic crypts isolated from β-catenin-inducible mice treated with a lower dose of doxycycline in drinking water (0.1 mg/ml) and found that the lower dose treatment significantly upregulated the expression of Wnt target genes such as *Myc*, but the same treatment did not induce *Lgr5* and *Hes1* in colonic crypts (supplementary material Fig. S9). Together, these results show that activation of the Notch signalling pathway and amplification of ISC-like cells require higher level of β-catenin accumulation. In addition, the expression of the Cdk inhibitors *Cdkn1a*, *Cdkn1b* and *Cdkn1c* were not altered by the lower level of β-catenin induction (supplementary material Fig. S9) in sharp contrast to the case of the higher level of β-catenin induction (supplementary material Fig. S5), suggesting that altered expression of Cdk inhibitors might be responsible for the different proliferative activities.

Colon tumors show heterogeneity in nuclear β-catenin expression and slow-cycling cells in the *Apc*$^{Min/+}$ mouse model

A large body of evidence indicates that accumulation of β-catenin is an initiating event in intestinal carcinogenesis (Harada et al., 1999; Yamada et al., 2002). The vast majority of colon cancers show accumulation of β-catenin and expression of elevated levels of β-catenin/Tcf target genes. However, strong nuclear accumulation of β-catenin is only observed in a subset of tumour cells, indicating heterogeneity of tumour cells within the tumour (Fodde and Brabletz, 2007). Similarly, we found that colon tumours in *Apc*$^{Min/+}$ mice, a well-established model for colon tumorigenesis, also show heterogeneous expression of nuclear β-catenin (Fig. 6A). To determine whether such heterogeneous expression of nuclear β-catenin affects downstream transcription of the canonical Wnt signalling, we examined colon tumours of *Apc*$^{Min/+}$ mice carrying a transgenic GFP reporter allele of β-catenin/Tcf transcription (Oyama et al., 2008). Double

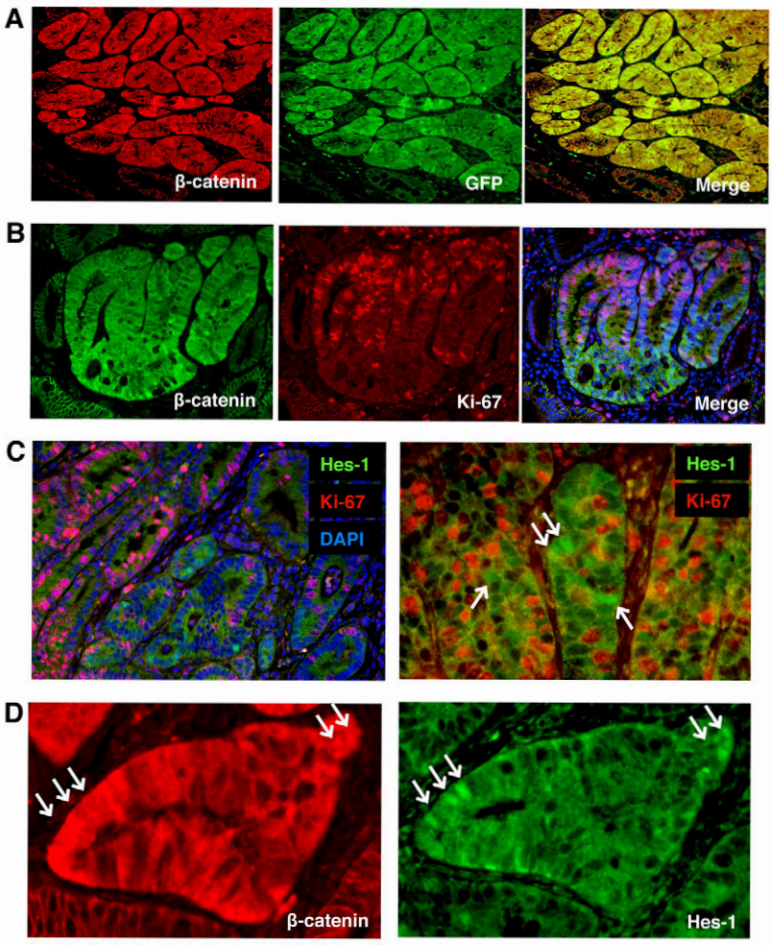

Fig. 6. Heterogeneity of colon tumour cells in *Apc*$^{Min/+}$ mouse. (**A**) Double immunostaining for β-catenin (red) and GFP (green) in the colon tumour of *Apc*$^{Min/+}$ mouse with transgenic GFP reporter allele for β-catenin/Tcf transcription activity. Note that heterogeneous expressions of both β-catenin and GFP are observed in a colon tumour. (**B**) Double immunostaining for β-catenin and Ki-67 in a colon tumour. Tumor cells with strong β-catenin expression show less frequent staining for Ki-67. (**C**) Double immunostaining for Hes1 (green) and Ki-67 (red). Distinct localisation of Hes1-expressing cells and Ki-67-positive cells are seen in colon tumour. Arrows indicate cells with positive nuclear staining for Hes1. (**D**) Immunostaining for β-catenin and Hes1 in serial sections. Colocalisation of higher levels of β-catenin and Hes1 expression is observed in the colon tumour.

immunofluorescence staining revealed that β-catenin levels were well correlated with GFP intensity, demonstrating that different levels of β-catenin accumulation directly affect β-catenin/Tcf transcription in colonic tumours (Fig. 6A). Importantly, most tumour cells with nuclear β-catenin did not express Ki-67 (Fig. 6B), recapitulating our observations in β-catenin-overexpressing mice. When the intensity and localisation of β-catenin expression were examined by immunofluorescence staining, the majority of Ki-67-positive tumour cells showed cytoplasmic β-catenin expression (93.6%) rather than strong nuclear expression (6.4%). In addition to the heterogeneous pattern of nuclear β-catenin accumulation, expression of Hes1 was detectable only in a small subset of colon tumour cells (Fig. 6C,D). Co-staining for Ki-67 revealed that tumour cells with high levels of Hes1 do not divide actively (Fig. 6C). Furthermore, we found that cells with a nuclear β-catenin signal often exhibited high Hes1 expression (Fig. 6D), as we have seen in β-catenin-induced crypts (supplementary material Fig. S4). These findings indicate that colon tumours, like our β-catenin inducible mouse model, consist of heterogeneous populations of cells displaying different activities of canonical Wnt signalling, Notch signalling and cell proliferation.

DISCUSSION

Previous studies using conditional *Apc* knockout mice demonstrated that acute loss of the *Apc* gene rapidly expands progenitor cells in the intestinal crypts (Sansom et al., 2004; Andreu et al., 2005) but does not lead to crypt fission/branching, suggesting that Wnt activation through loss of *Apc* is not sufficient to induce *de novo* crypt formation. In the present study, we showed that high levels of β-catenin activation are sufficient for *de novo* crypt formation of adult mice (Fig. 2). Our observation suggests that β-catenin activation amplifies ISCs, which is consistent with recent work carried out in *Drosophila* hindgut (Takashima et al., 2008). The discrepancy between previous reports and our study seems to arise from differences in the levels of Wnt activation. In fact, by titrating down the levels of activated β-catenin, we also failed to induce *de novo* crypt formation but instead expanded the proliferating progenitor compartment of the crypts (Fig. 5A). These combined findings strongly suggest that high levels of the canonical Wnt effector β-catenin are required for ISC expansion, whereas low levels of activation can induce the active proliferation of progenitor cells. This notion is consistent with a recent finding, which demonstrated that different levels of Wnt signalling exert distinct roles on the self-renewal and differentiation potentials of haematopoietic stem cells (Luis et al., 2011).

The notion that *de novo* crypt formation and cell proliferation are controlled by distinct levels of β-catenin activation is reminiscent of previous observations from our laboratory on the two-stage tumorigenesis of the *Apc*$^{Min/+}$ mouse (Yamada et al., 2002; Oyama et al., 2008). In the colon of *Apc*$^{Min/+}$ mice, we detected many microadenomas as early as 3 weeks of age, of which only a limited number progressed to large tumours. Although early

microadenomas already harboured frequent loss of *Apc* and increased β-catenin/Tcf transcription, larger tumours exhibited further elevations of β-catenin/Tcf transcriptional activity, thus suggesting that increased β-catenin/Tcf signalling is required for the development of larger tumours. The dose-dependent effect of Wnt activation on intestinal tumorigenesis has also been implicated in mouse models with different hypomorphic *Apc* mutant alleles, supporting the requirement for higher levels of Wnt activation for intestinal tumorigenesis (Gaspar and Fodde, 2004). A series of previous studies demonstrated that epigenetic modifications associated with DNA methylation are involved in the transition from microadenomas to large tumours in the $Apc^{Min/+}$ mouse (Yamada et al., 2005; Lin et al., 2006; Linhart et al., 2007). In human colorectal cancers, it has been shown that epigenetic silencing of SFRPs, negative modifiers of Wnt signalling, are frequently found, and such inactivation can further activate the canonical Wnt signals in colon cancer cell lines with *APC* or *CTNNB1* mutations (Suzuki et al., 2004). It is therefore possible that activation of the canonical Wnt signalling by both genetic and epigenetic alterations enables colonic stem cells to expand, leading to *de novo* crypt formation, which ultimately results in tumour growth.

A number of signalling cascades have been implicated in the maintenance of intestinal homeostasis (Scoville et al., 2008), but it remains unclear how the Wnt signalling pathway connects with other signalling cascades within the intestine to control homeostasis. Here, we showed that canonical Wnt signalling plays an important role in *de novo* crypt formation in the colon, and that a higher level of β-catenin activation is crucial for Notch activation. Our finding that Notch inhibition prevented crypt fission/branching in β-catenin-induced colon indicates the requirement for Notch activation in β-catenin-induced *de novo* crypt formation (Fig. 4G; supplementary material Fig. S8A). Interestingly, β-catenin activation rapidly induced transcriptional activation of the Notch ligands *Jag1* and *Jag2*, and the Notch receptors *Notch1* and *Notch2* (Fig. 4B, Fig. 5B), thus offering a possible direct link between these two pathways. Together with previous findings that β-catenin induces *Jag1* transcription, leading to Notch activation in human colon cancer cell lines (Rodilla et al., 2009), it is therefore likely that the increased expression of Notch ligands by β-catenin induction causes Notch activation in the colonic epithelium. Furthermore, a recent study clearly demonstrated that Notch1 and Notch2 receptors are expressed specifically in ISCs (Fre et al., 2011; Sato et al., 2011). The increased expressions of Notch receptors could play a role in the induction of ISC-like cells by β-catenin induction (Fig. 4B). It is also noteworthy that the constitutive activation of Notch results in no obvious effect on β-catenin nuclear localisation (Fre et al., 2005). These findings indicate a hierarchical relationship between the Wnt and Notch signalling pathways in the intestinal epithelium. This hierarchy might explain why genetic alterations in colon cancers are frequently detected in the Wnt signalling pathway, but not in the Notch signalling pathway.

The failure of most current therapies to cure cancer has led to the hypothesis that treatments targeted at malignant proliferation spare a slowly cycling cancer stem cell population. In this study, higher levels of Wnt activation induced *de novo* crypt formation and induced crypt cells to acquire slow-cycling properties. Interestingly, our observation of a β-catenin-induced slow-cycling property is consistent with previous reports in human colorectal cancers. Human colourectal cancers showed heterogeneous intracellular distribution of β-catenin, and tumour cells with nuclear accumulation revealed low cell proliferation rates (Brabletz et al., 2001; Fodde and Brabletz, 2007). Importantly, we also found that colon tumours in $Apc^{Min/+}$ mice consist of heterogeneous cells displaying different levels of β-catenin accumulation and downstream gene expression (Fig. 6A), and tumour cells with nuclear β-catenin are dividing more slowly than surrounding tumour cells, suggesting that such cells are similar to cells at the crypt bottom of the normal colon. Thus, we propose that a hierarchical control of cell proliferation in the colonic crypt epithelium is retained to some extent in colonic neoplasms. Accordingly, we found that tumour cells with nuclear β-catenin are accompanied by high Notch signalling (Fig. 6D), as has been reported in crypt bottom cells (Kayahara et al., 2003). It is interesting to note that a γ-secretase inhibitor turned slow-cycling cells into actively proliferating cells (Fig. 4C-G; supplementary material Fig. S7A). A previous study showed that Notch inhibitors turn undifferentiated, proliferating cells into quiescent cells in colorectal neoplasias (van Es et al., 2005), indicating that the Notch inhibitor might be of therapeutic benefit in colorectal cancers. The discrepancy in the effects of Notch inhibitor could be explained by differences in states of the affected cells between proliferating progenitor cells and ISC-like cells. Although the previous study showed effects on the transition of proliferating cells into terminally differentiated quiescent cells, our data suggest that a Notch inhibitor may promote the transition of slow-cycling ISC-like cells into progenitor cells in the colon. Considering the chemoresistance of slow-cycling cancer stem cells, the results also suggest that Notch inhibitors combined with chemotherapeutic agents and/or irradiation might be effective as treatments targeting slow-cycling cancer stem cells in the colon.

In summary, our results indicate that, although proliferating progenitor cells in colonic crypts physiologically express higher levels of β-catenin/Tcf transcriptions, a further activation of the canonical Wnt singalling leads to *de novo* crypt formation, consisting of relatively slow-cycling cells in the adult colon, which is accompanied by activation of Notch signalling with transactivation of Notch ligands and receptors. However, treatment with a Notch/γ-secretase inhibitor turns such slow-cycling cells into proliferating cells, although we cannot exclude the possibility that some of the observed phenotypes are the result of superphysiological β-catenin expression obtained with our transgenic system. These findings suggest that Wnt and Notch signalling act in a synergistic and hierarchical manner to control differentiation and proliferation of the colonic crypt epithelium *in vivo*.

Acknowledgements
We thank Ayako Suga, Kyoko Takahashi, Huilan Zhi and Yoshitaka Kinjyo for technical assistance, and Hans Clevers for providing the S33 β-catenin overexpression vector.

Funding
This study is supported by PRESTO, Grants-in-Aid from the Ministry of Health, Labour and Welfare of Japan, and Ministry of Education, Culture, Sports, Science and Technology of Japan [Y.Y.]. J.U. is supported by grants of the German Cancer Aid and German Research Council [SFB873]. K.H. was supported by the National Institutes of Health [DP2OD003266 and R01HD058013]. Deposited in PMC for release after 12 months.

Competing interests statement
The authors declare no competing financial interests.

Supplementary material
Supplementary material available online at
http://dev.biologists.org/lookup/suppl/doi:10.1242/dev.084103/-/DC1

References

Andreu, P., Colnot, S., Godard, C., Gad, S., Chafey, P., Niwa-Kawakita, M., Laurent-Puig, P., Kahn, A., Robine, S., Perret, C. et al. (2005). Crypt-restricted proliferation and commitment to the Paneth cell lineage following Apc loss in the mouse intestine. *Development* **132**, 1443-1451.

Barker, N., van Es, J. H., Kuipers, J., Kujala, P., van den Born, M., Cozijnsen, M., Haegebarth, A., Korving, J., Begthel, H., Peters, P. J. et al. (2007). Identification of stem cells in small intestine and colon by marker gene Lgr5. *Nature* **449**, 1003-1007.
Beard, C., Hochedlinger, K., Plath, K., Wutz, A. and Jaenisch, R. (2006). Efficient method to generate single-copy transgenic mice by site-specific integration in embryonic stem cells. *Genesis* **44**, 23-28.
Brabletz, T., Jung, A., Reu, S., Porzner, M., Hlubek, F., Kunz-Schughart, L. A., Knuechel, R. and Kirchner, T. (2001). Variable beta-catenin expression in colorectal cancers indicates tumor progression driven by the tumor environment. *Proc. Natl. Acad. Sci. USA* **98**, 10356-10361.
Fevr, T., Robine, S., Louvard, D. and Huelsken, J. (2007). Wnt/beta-catenin is essential for intestinal homeostasis and maintenance of intestinal stem cells. *Mol. Cell. Biol.* **27**, 7551-7559.
Fodde, R. and Brabletz, T. (2007). Wnt/beta-catenin signaling in cancer stemness and malignant behavior. *Curr. Opin. Cell Biol.* **19**, 150-158.
Foudi, A., Hochedlinger, K., Van Buren, D., Schindler, J. W., Jaenisch, R., Carey, V. and Hock, H. (2009). Analysis of histone 2B-GFP retention reveals slowly cycling hematopoietic stem cells. *Nat. Biotechnol.* **27**, 84-90.
Fre, S., Huyghe, M., Mourikis, P., Robine, S., Louvard, D. and Artavanis-Tsakonas, S. (2005). Notch signals control the fate of immature progenitor cells in the intestine. *Nature* **435**, 964-968.
Fre, S., Hannezo, E., Sale, S., Huyghe, M., Lafkas, D., Kissel, H., Louvi, A., Greve, J., Louvard, D. and Artavanis-Tsakonas, S. (2011). Notch lineages and activity in intestinal stem cells determined by a new set of knock-in mice. *PLoS ONE* **6**, e25785.
Gaspar, C. and Fodde, R. (2004). APC dosage effects in tumorigenesis and stem cell differentiation. *Int. J. Dev. Biol.* **48**, 377-386.
Harada, N., Tamai, Y., Ishikawa, T., Sauer, B., Takaku, K., Oshima, M. and Taketo, M. M. (1999). Intestinal polyposis in mice with a dominant stable mutation of the beta-catenin gene. *EMBO J.* **18**, 5931-5942.
He, X. C., Yin, T., Grindley, J. C., Tian, Q., Sato, T., Tao, W. A., Dirisina, R., Porter-Westpfahl, K. S., Hembree, M., Johnson, T. et al. (2007). PTEN-deficient intestinal stem cells initiate intestinal polyposis. *Nat. Genet.* **39**, 189-198.
Ito, T., Udaka, N., Yazawa, T., Okudela, K., Hayashi, H., Sudo, T., Guillemot, F., Kageyama, R. and Kitamura, H. (2000). Basic helix-loop-helix transcription factors regulate the neuroendocrine differentiation of fetal mouse pulmonary epithelium. *Development* **127**, 3913-3921.
Jung, A., Schrauder, M., Oswald, U., Knoll, C., Sellberg, P., Palmqvist, R., Niedobitek, G., Brabletz, T. and Kirchner, T. (2001). The invasion front of human colorectal adenocarcinomas shows co-localization of nuclear beta-catenin, cyclin D1, and p16INK4A and is a region of low proliferation. *Am. J. Pathol.* **159**, 1613-1617.
Kaneko, Y., Sakakibara, S., Imai, T., Suzuki, A., Nakamura, Y., Sawamoto, K., Ogawa, Y., Toyama, Y., Miyata, T. and Okano, H. (2000). Musashi1: an evolutionally conserved marker for CNS progenitor cells including neural stem cells. *Dev. Neurosci.* **22**, 139-153.
Kayahara, T., Sawada, M., Takaishi, S., Fukui, H., Seno, H., Fukuzawa, H., Suzuki, K., Hiai, H., Kageyama, R., Okano, H. et al. (2003). Candidate markers for stem and early progenitor cells, Musashi-1 and Hes1, are expressed in crypt base columnar cells of mouse small intestine. *FEBS Lett.* **535**, 131-135.
Korinek, V., Barker, N., Moerer, P., van Donselaar, E., Huls, G., Peters, P. J. and Clevers, H. (1998). Depletion of epithelial stem-cell compartments in the small intestine of mice lacking Tcf-4. *Nat. Genet.* **19**, 379-383.
Kuhnert, F., Davis, C. R., Wang, H. T., Chu, P., Lee, M., Yuan, J., Nusse, R. and Kuo, C. J. (2004). Essential requirement for Wnt signaling in proliferation of adult small intestine and colon revealed by adenoviral expression of Dickkopf-1. *Proc. Natl. Acad. Sci. USA* **101**, 266-271.
Li, L. and Clevers, H. (2010). Coexistence of quiescent and active adult stem cells in mammals. *Science* **327**, 542-545.
Lin, H., Yamada, Y., Nguyen, S., Linhart, H., Jackson-Grusby, L., Meissner, A., Meletis, K., Lo, G. and Jaenisch, R. (2006). Suppression of intestinal neoplasia by deletion of Dnmt3b. *Mol. Cell. Biol.* **26**, 2976-2983.
Linhart, H. G., Lin, H., Yamada, Y., Moran, E., Steine, E. J., Gokhale, S., Lo, G., Cantu, E., Ehrich, M., He, T. et al. (2007). Dnmt3b promotes tumorigenesis *in vivo* by gene-specific *de novo* methylation and transcriptional silencing. *Genes Dev.* **21**, 3110-3122.
Luis, T. C., Naber, B. A., Roozen, P. P., Brugman, M. H., de Haas, E. F., Ghazvini, M., Fibbe, W. E., van Dongen, J. J., Fodde, R. and Staal, F. J. (2011). Canonical wnt signaling regulates hematopoiesis in a dosage-dependent fashion. *Cell Stem Cell* **9**, 345-356.
Morin, P. J., Sparks, A. B., Korinek, V., Barker, N., Clevers, H., Vogelstein, B. and Kinzler, K. W. (1997). Activation of beta-catenin-Tcf signaling in colon cancer by mutations in beta-catenin or AP. *Science* **275**, 1787-1790.
Oyama, T., Yamada, Y., Hata, K., Tomita, H., Hirata, A., Sheng, H., Hara, A., Aoki, H., Kunisada, T., Yamashita, S. et al. (2008). Further upregulation of beta-catenin/Tcf transcription is involved in the development of macroscopic tumors in the colon of ApcMin/+ mice. *Carcinogenesis* **29**, 666-672.
Pinto, D., Gregorieff, A., Begthel, H. and Clevers, H. (2003). Canonical Wnt signals are essential for homeostasis of the intestinal epithelium. *Genes Dev.* **17**, 1709-1713.
Potten, C. S., Booth, C., Tudor, G. L., Booth, D., Brady, G., Hurley, P., Ashton, G., Clarke, R., Sakakibara, S. and Okano, H. (2003). Identification of a putative intestinal stem cell and early lineage marker; musashi-1. *Differentiation* **71**, 28-41.
Rodilla, V., Villanueva, A., Obrador-Hevia, A., Robert-Moreno, A., Fernández-Majada, V., Grilli, A., López-Bigas, N., Bellora, N., Albà, M. M., Torres, F. et al. (2009). Jagged1 is the pathological link between Wnt and Notch pathways in colorectal cancer. *Proc. Natl. Acad. Sci. USA* **106**, 6315-6320.
Sangiorgi, E. and Capecchi, M. R. (2008). Bmi1 is expressed *in vivo* in intestinal stem cells. *Nat. Genet.* **40**, 915-920.
Sansom, O. J., Reed, K. R., Hayes, A. J., Ireland, H., Brinkmann, H., Newton, I. P., Batlle, E., Simon-Assmann, P., Clevers, H., Nathke, I. S. et al. (2004). Loss of Apc *in vivo* immediately perturbs Wnt signaling, differentiation, and migration. *Genes Dev.* **18**, 1385-1390.
Sato, T., van Es, J. H., Snippert, H. J., Stange, D. E., Vries, R. G., van den Born, M., Barker, N., Shroyer, N. F., van de Wetering, M. and Clevers, H. (2011). Paneth cells constitute the niche for Lgr5 stem cells in intestinal crypts. *Nature* **469**, 415-418.
Scoville, D. H., Sato, T., He, X. C. and Li, L. (2008). Current view: intestinal stem cells and signaling. *Gastroenterology* **134**, 849-864.
Suzuki, H., Watkins, D. N., Jair, K. W., Schuebel, K. E., Markowitz, S. D., Chen, W. D., Pretlow, T. P., Yang, B., Akiyama, Y., Van Engeland, M. et al. (2004). Epigenetic inactivation of SFRP genes allows constitutive WNT signaling in colorectal cancer. *Nat. Genet.* **36**, 417-422.
Takashima, S., Mkrtchyan, M., Younossi-Hartenstein, A., Merriam, J. R. and Hartenstein, V. (2008). The behaviour of Drosophila adult hindgut stem cells is controlled by Wnt and Hh signalling. *Nature* **454**, 651-655.
Takeda, N., Jain, R., LeBoeuf, M. R., Wang, Q., Lu, M. M. and Epstein, J. A. (2011). Interconversion between intestinal stem cell populations in distinct niches. *Science* **334**, 1420-1424.
Tsukamoto, T., Fukami, H., Yamanaka, S., Yamaguchi, A., Nakanishi, H., Sakai, H., Aoki, I. and Tatematsu, M. (2001). Hexosaminidase-altered aberrant crypts, carrying decreased hexosaminidase alpha and beta subunit mRNAs, in colon of 1,2-dimethylhydrazine-treated rats. *Jpn. J. Cancer Res.* **92**, 109-118.
Tumbar, T., Guasch, G., Greco, V., Blanpain, C., Lowry, W. E., Rendl, M. and Fuchs, E. (2004). Defining the epithelial stem cell niche in skin. *Science* **303**, 359-363.
van de Wetering, M., Sancho, E., Verweij, C., de Lau, W., Oving, I., Hurlstone, A., van der Horn, K., Batlle, E., Coudreuse, D., Haramis, A. P. et al. (2002). The beta-catenin/TCF-4 complex imposes a crypt progenitor phenotype on colorectal cancer cells. *Cell* **111**, 241-250.
van der Flier, L. G., Sabates-Bellver, J., Oving, I., Haegebarth, A., De Palo, M., Anti, M., Van Gijn, M. E., Suijkerbuijk, S., Van de Wetering, M., Marra, G. et al. (2007). The Intestinal Wnt/TCF Signature. *Gastroenterology* **132**, 628-632.
van der Flier, L. G., van Gijn, M. E., Hatzis, P., Kujala, P., Haegebarth, A., Stange, D. E., Begthel, H., van den Born, M., Guryev, V., Oving, I. et al. (2009). Transcription factor achaete scute-like 2 controls intestinal stem cell fate. *Cell* **136**, 903-912.
van Es, J. H., van Gijn, M. E., Riccio, O., van den Born, M., Vooijs, M., Begthel, H., Cozijnsen, M., Robine, S., Winton, D. J., Radtke, F. et al. (2005). Notch/gamma-secretase inhibition turns proliferative cells in intestinal crypts and adenomas into goblet cells. *Nature* **435**, 959-963.
van Noort, M., van de Wetering, M. and Clevers, H. (2002). Identification of two novel regulated serines in the N terminus of beta-catenin. *Exp. Cell Res.* 276, 264-272.
Vermeulen, L., De Sousa E Melo, F., van der Heijden, M., Cameron, K., de Jong, J. H., Borovski, T., Tuynman, J. B., Todaro, M., Merz, C., Rodermond, H. et al. (2010). Wnt activity defines colon cancer stem cells and is regulated by the microenvironment. *Nat. Cell Biol.* **12**, 468-476.
Yamada, Y., Hata, K., Hirose, Y., Hara, A., Sugie, S., Kuno, T., Yoshimi, N., Tanaka, T. and Mori, H. (2002). Microadenomatous lesions involving loss of Apc heterozygosity in the colon of adult Apc(Min/+) mice. *Cancer Res.* **62**, 6367-6370.
Yamada, Y., Jackson-Grusby, L., Linhart, H., Meissner, A., Eden, A., Lin, H. and Jaenisch, R. (2005). Opposing effects of DNA hypomethylation on intestinal and liver carcinogenesis. *Proc. Natl. Acad. Sci. USA* **102**, 13580-13585.
Yamashita, S., Nomoto, T., Ohta, T., Ohki, M., Sugimura, T. and Ushijima, T. (2003). Differential expression of genes related to levels of mucosal cell proliferation among multiple rat strains by using oligonucleotide microarrays. *Mamm. Genome* **14**, 845-852.

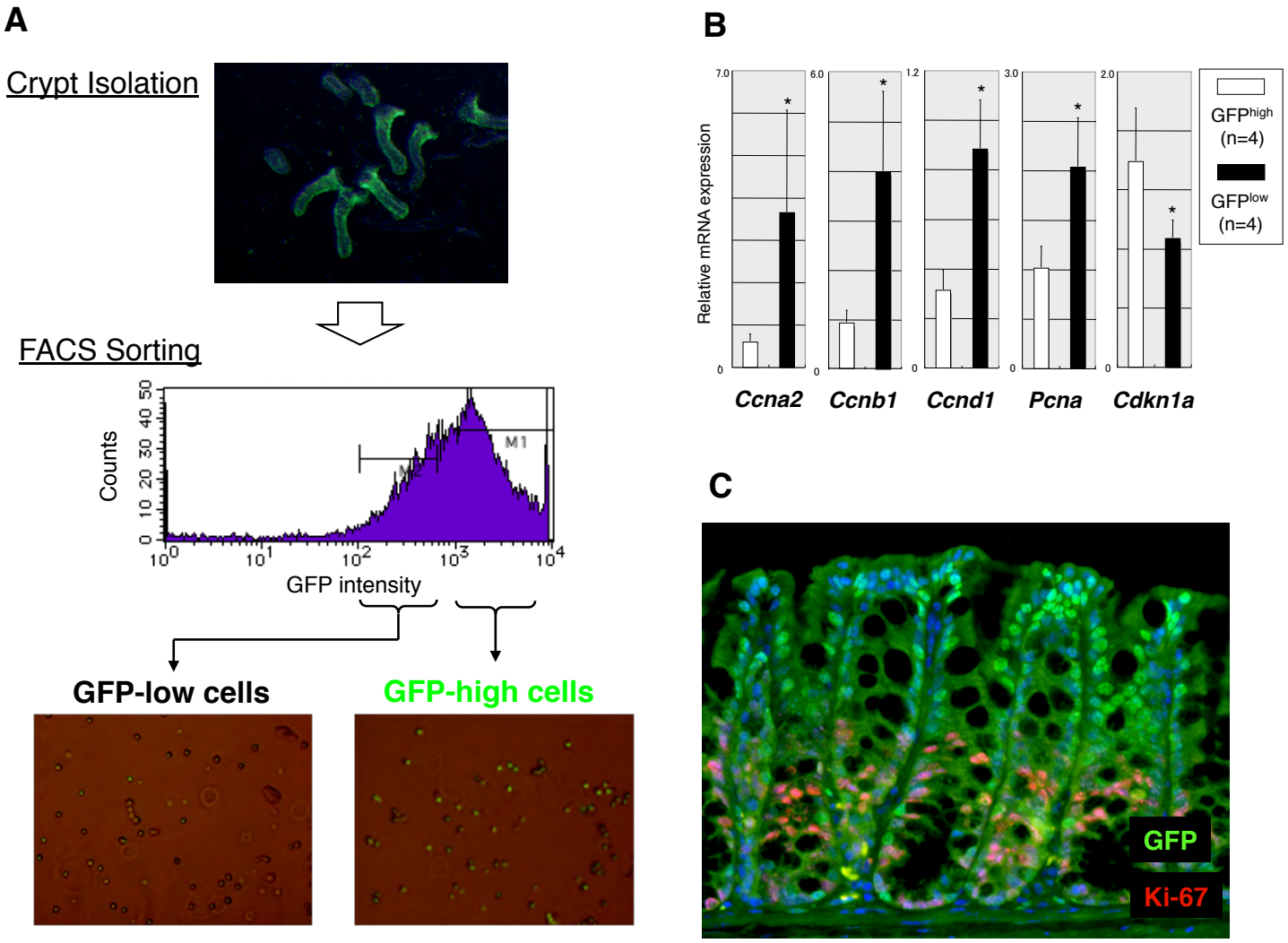

Fig. S1. Separation of proliferating cells from non-proliferative cells in the colon of histone H2B-GFP inducible mice. (**A**) Schematic of separation of proliferating cells from non-proliferating cells in the colonic crypts. GFP^{high} and GFP^{low} cells were sorted from the isolated crypts by FACS. (**B**) Expression of cell cycle-related genes assessed by quantitative real-time PCR. The expressions of *Ccna2*, *Ccnb1*, *Ccnd1* and *Pcna* were significantly higher in GFP^{low} proliferating cells than in GFP^{high} non-proliferating cells, whereas the expression of *Cdkn1a* (*p21*) was significantly upregulated in GFP^{high} cells. Data represent means ± s.d.; **P*<0.05, by Mann–Whitney *U*-test. (**C**) Immunostaining for GFP (green) and Ki-67 (red) on a colon section of anH2B-GFP inducible mouse. GFP^{low} cells contain a higher number of Ki-67-positive cells than do GFP^{high} cells.

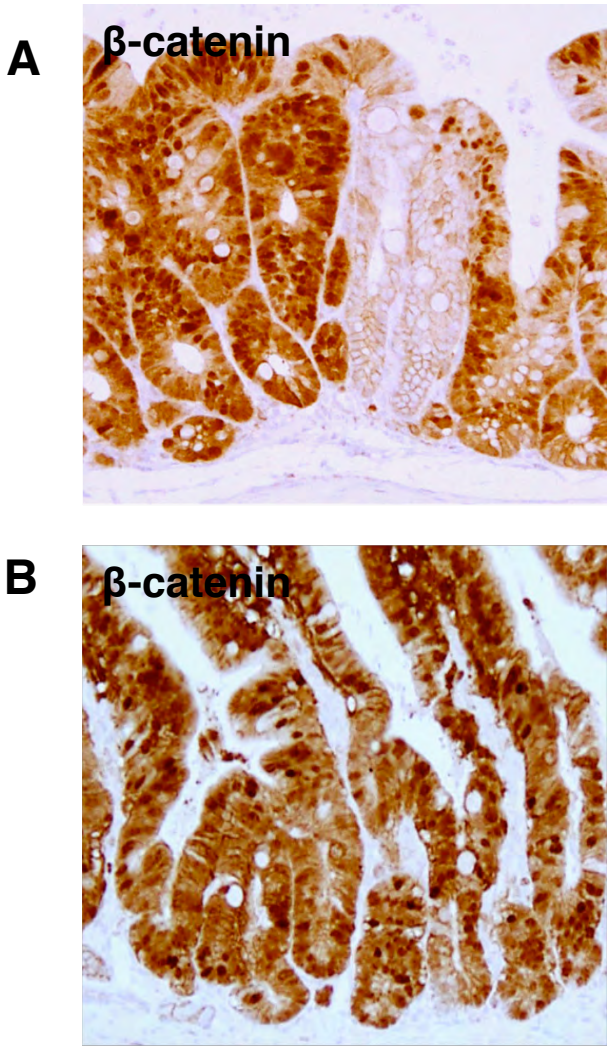

Fig. S2. Forced expression of β-catenin leads to crypt fission in both colon and small intestine. (**A**) Immunostaining for β-catenin on colonic section of a doxycycline-treated chimeric mouse. Crypt fission/branching phenotype is detectable only in β-catenin-induced crypts but not in host embryo-derived crypts. (**B**) Immunostaining for β-catenin in the small intestine of a β-catenin-induced mouse. β-Catenin induction causes frequent crypt fission/branching also in crypts of small intestine.

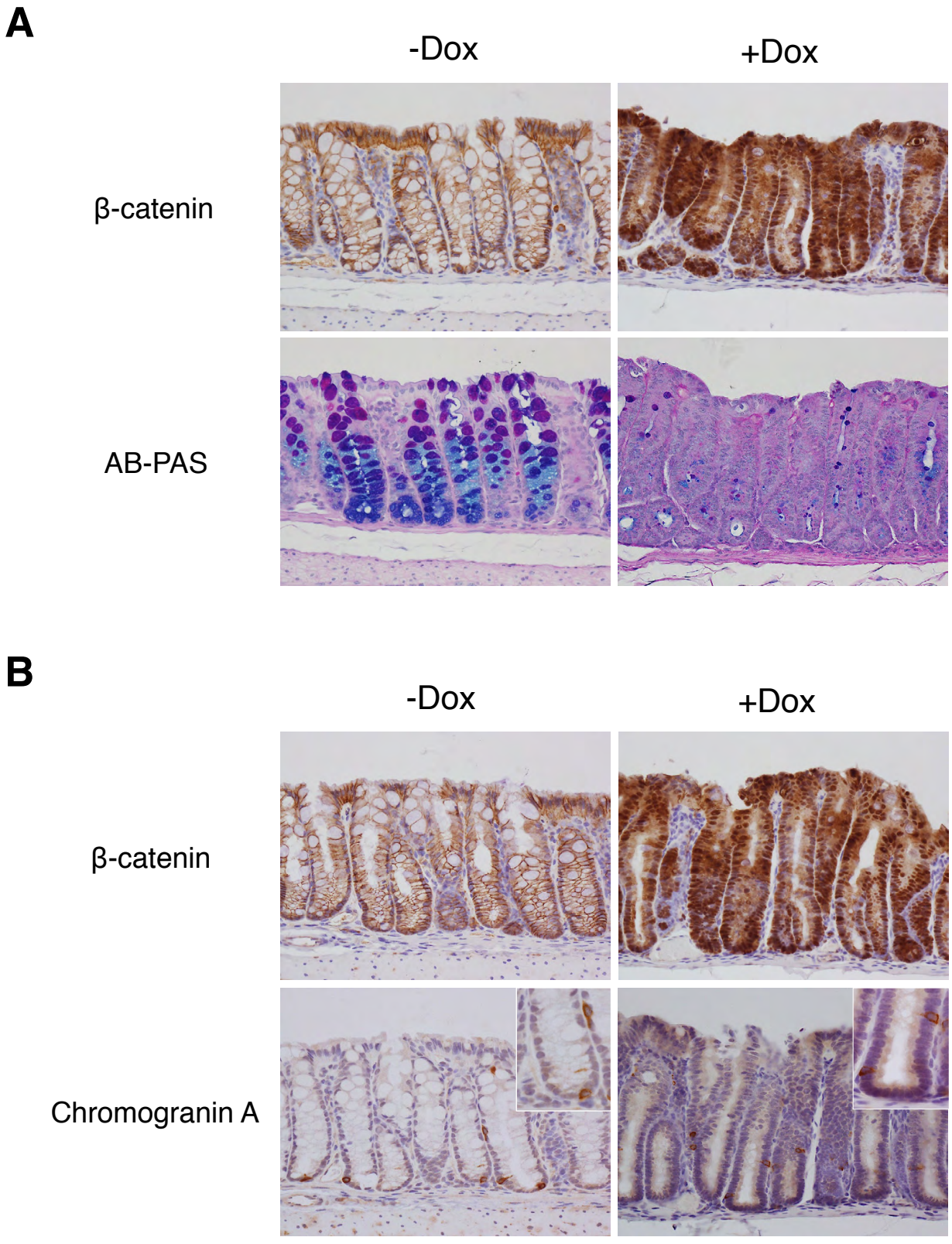

Fig. S3. Effect of β-catenin induction on differentiation of colonic epithelial cells. (**A**) Immunostaining for β-catenin and Alcian-Blue-periodic acid-Schiff (AB-PAS) staining on serial colonic sections of untreated and doxycycline-treated β-catenin inducible mice. Mucin-producing goblet cells were markedly reduced in β-catenin-induced colon. (**B**) Immunostaining for β-catenin and chromogranin A on serial colonic sections of untreated and doxycycline-treated β-catenin inducible mice. Chromogranin A-positive enteroendocrine cells were found in both β-catenin induced and non-induced crypts. Insets show higher magnification views of colonic crypts.

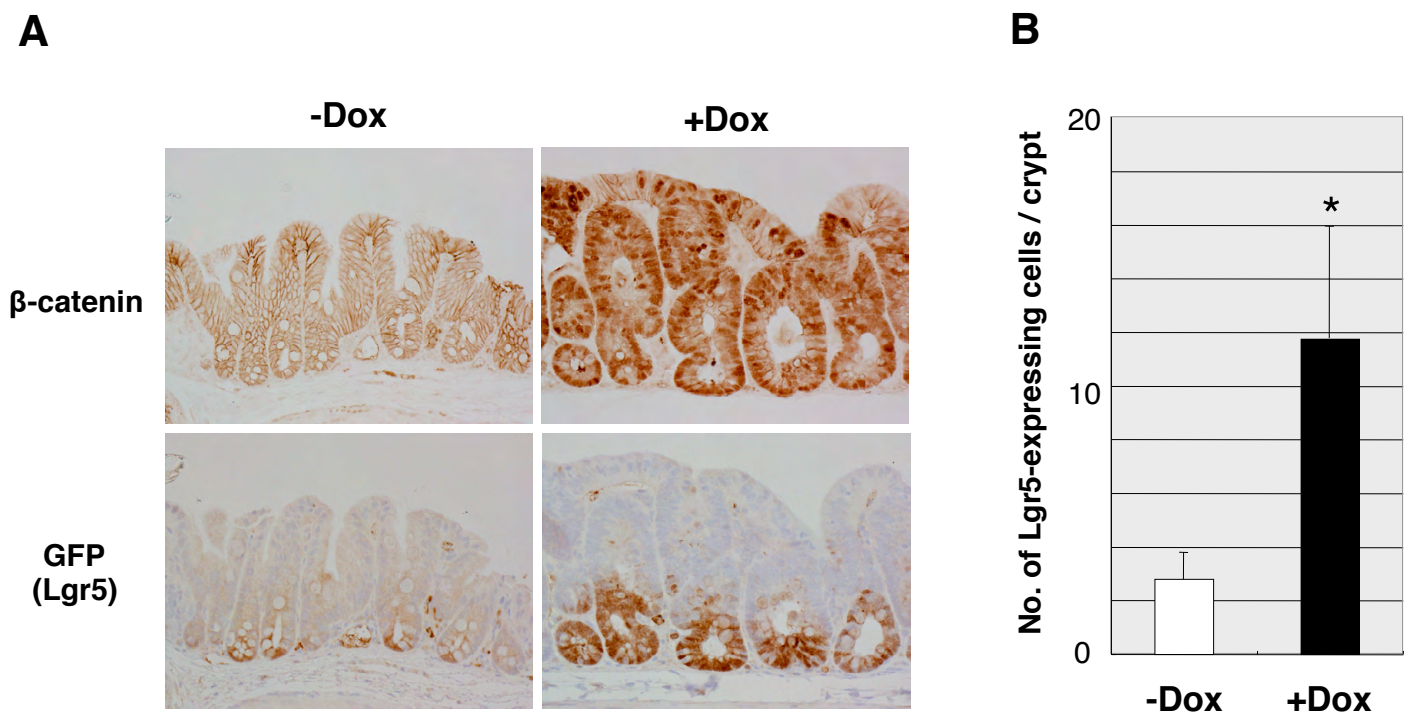

Fig. S4. Forced expression of β-catenin increases the number of *Lgr5*-expressing cells in colonic crypts. (**A**) Immunostaining for β-catenin and GFP on colonic sections of β-catenin-induced mice with *Lgr5-GFP* knock-in allele. GFP expression reveals an increased number of *Lgr5*-expressing cells at the lower part of colonic crypts in β-catenin-induced mice. Note that *Lgr5*-expressing cells were only observed at the lower part of the colonic crypts (lower right) whereas nuclear accumulation of β-catenin was observed in the entire crypt epithelium (upper right). (**B**) The number of *Lgr5*-expressing cells per crypt in β-catenin-induced colon. The number of *Lgr5*-expressing cells significantly increases following β-catenin induction. Data represent mean ± s.d.; **P*<0.0001, by Student's *t*-test.

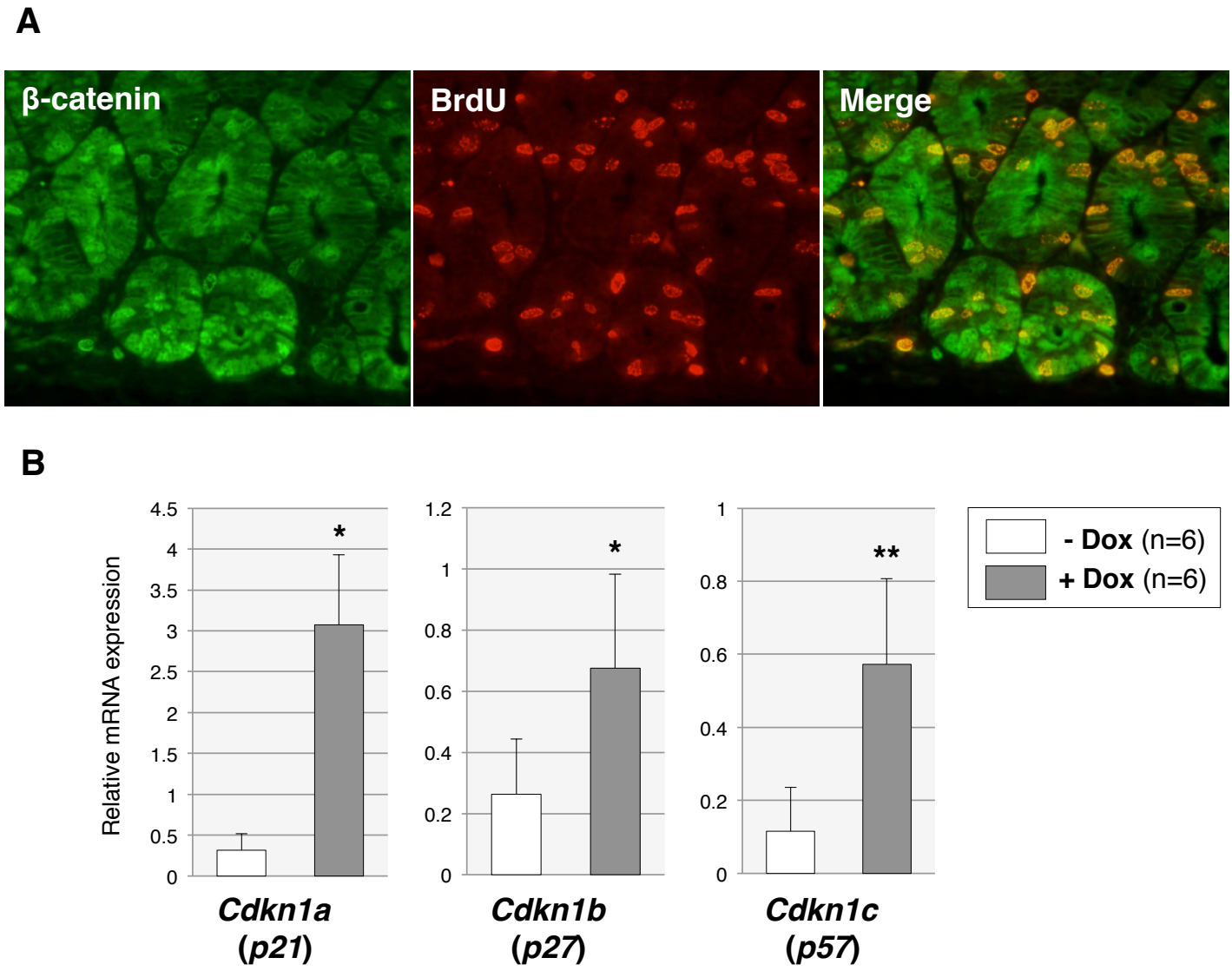

Fig. S5. Colonic cells with strong nuclear β-catenin expression do not actively divide. (**A**) Double immunostaining for β-catenin (green) and BrdU (red) on colonic section of a β-catenin-induced mouse given BrdU injection 2 hours before sacrifice. Colonic cells with strong nuclear β-catenin expression show less frequent BrdU incorporation. (**B**) Expression of cell Cdk inhibitors assessed by qRT-PCR. The expression of Cdk inhibitors is significantly upregulated by β-catenin induction. Data represent mean ± s.d.; **P*<0.05, ***P*<0.01 by Mann–Whitney *U*-test.

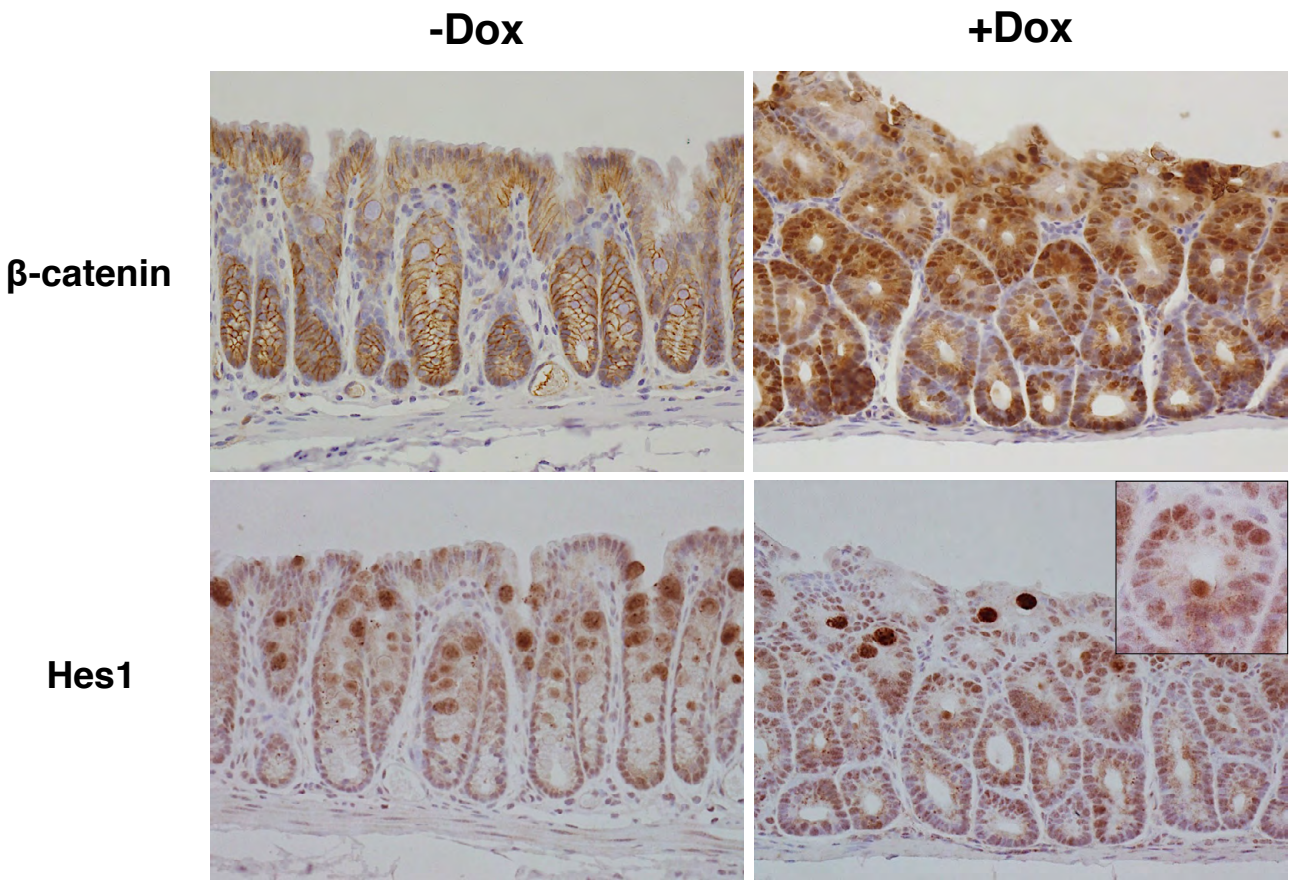

Fig. S6. Forced expression of β-catenin increases Hes1 expression in colonic crypts. Immunostaining for Hes1 on serial colonic sections of untreated and doxycycline-treated β-catenin-inducible mice. Strong nuclear expression of Hes1 is found in β-catenin-induced colonic crypts. Nuclear Hes1 can be observed throughout the crypt with β-catenin induction. Inset shows higher magnification views of β-catenin-induced crypts.

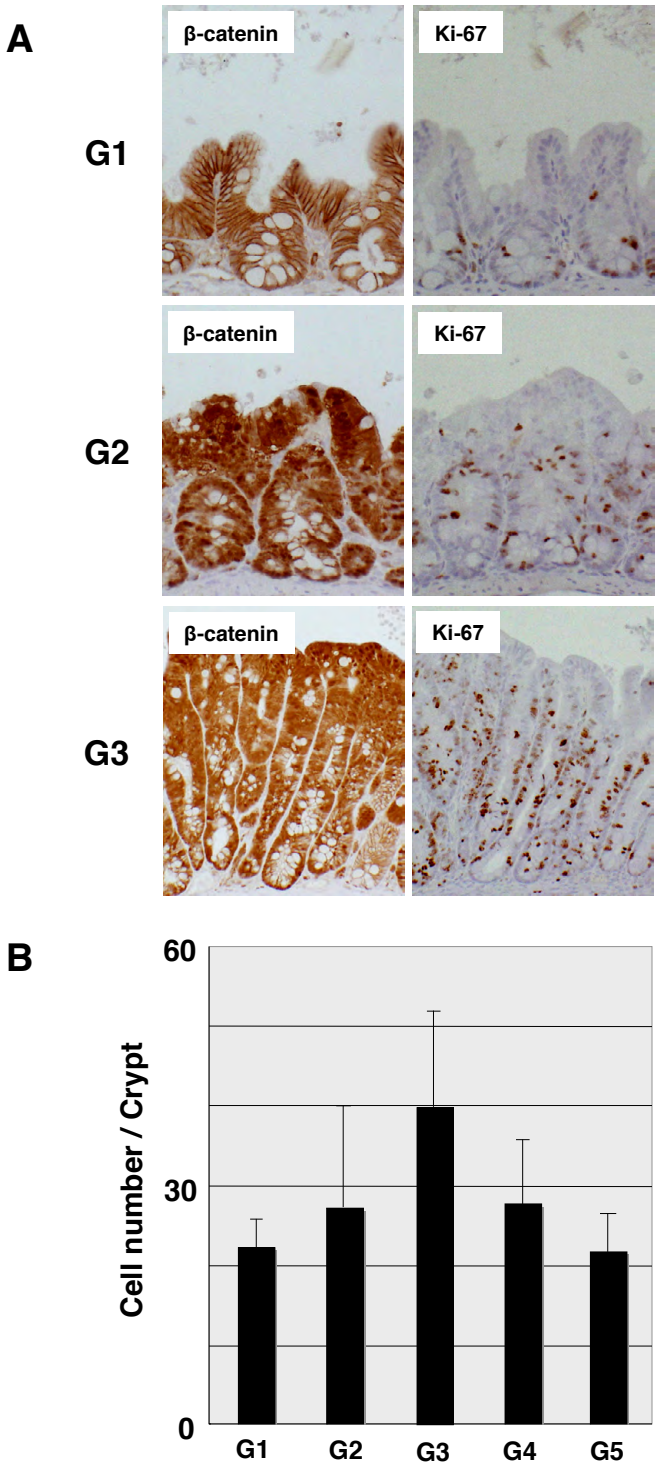

Fig. S7. Notch inhibitor induces active proliferation in the slow-cycling β-catenin induced colon. (**A**) Immunostaining for β-catenin and Ki-67 on colon sections. Treatment with a Notch inhibitor induces active cell proliferation of β-catenin-expressing cells. (**B**) The number of cells per crypt is significantly higher in G3 than other groups ($P<0.001$ for G1, $P<0.05$ for G2 and G4, and $P<0.0005$ for G5, respectively, by one-way ANOVA and Turkey's post hoc test), indicating elongation of the crypts. See Fig. 4 for description of protocols G1-G5.

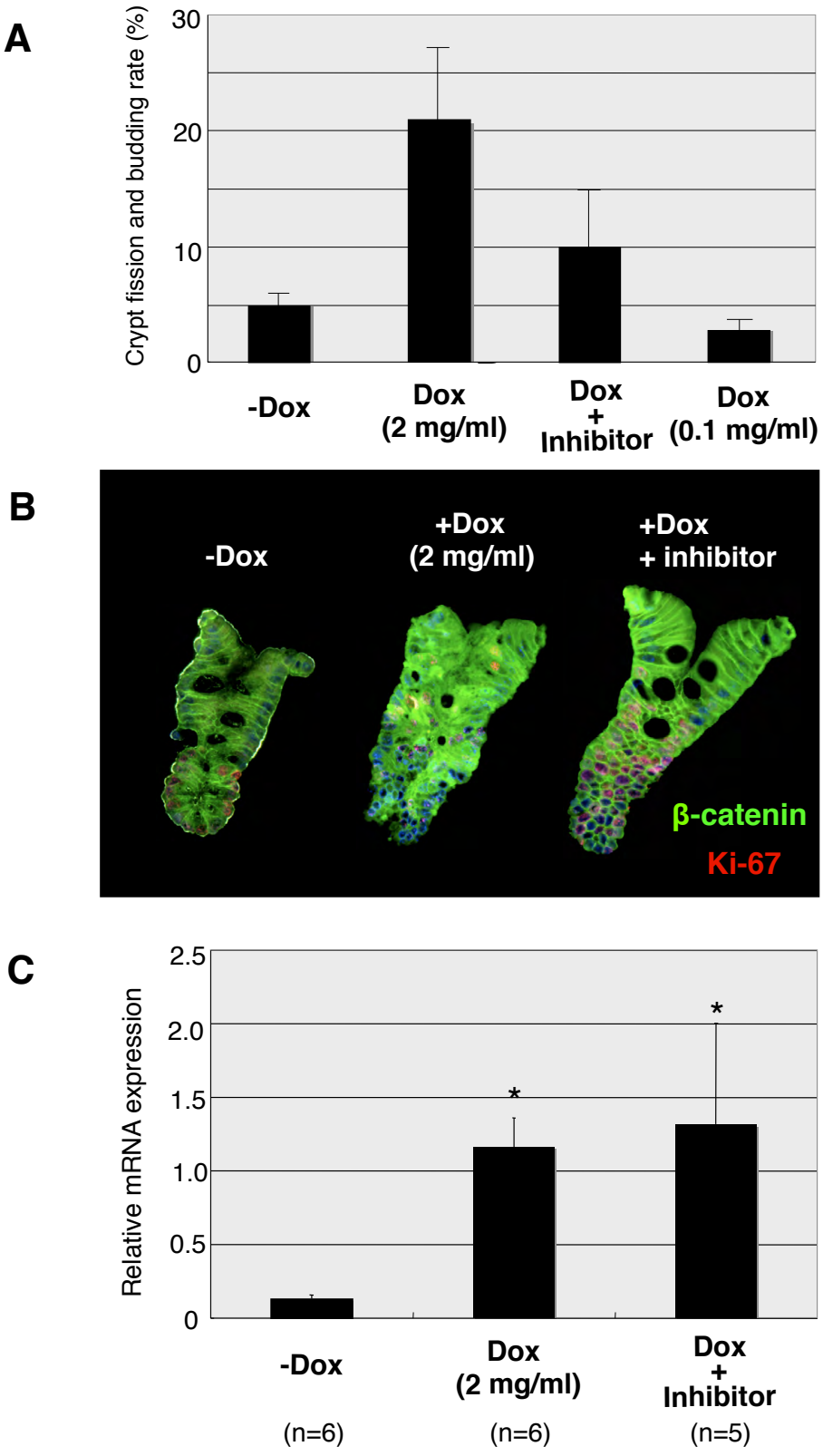

Fig. S8. Notch inhibitor suppresses the *de novo* crypt formation in β-catenin induced colon. (**A**) Crypt fission/budding rate of isolated crypts. The rate is significantly decreased at β-catenin-induced crypts with an inhibitor [$P<0.05$ compared with doxycyclin-treated mice (2 mg/ml), by Kruskal-Wallis test followed by Steel-Dwass test]. When mice are treated with lower concentration of doxycycline (0.1 mg/ml), the crypt fission/budding rate does not increase. (**B**) Double immunostaining for β-catenin (green) and Ki-67 (red) of isolated crypts. Treatment with a Notch inhibitor decreases nuclear β-catenin expression in β-catenin-induced crypt, which is accompanied by increased Ki-67 staining. (**C**) Quantitative real-time PCR for the gene encoding β-catenin. Notch inhibitor does not change β-catenin expression at the level of mRNA transcription in doxycyline-treated mice ($P=0.98$). Data represent mean ± s.d.; *$P<0.05$ compared with non-treated mice, by Kruskal-Wallis test and post-hoc Steel-Dwass test.

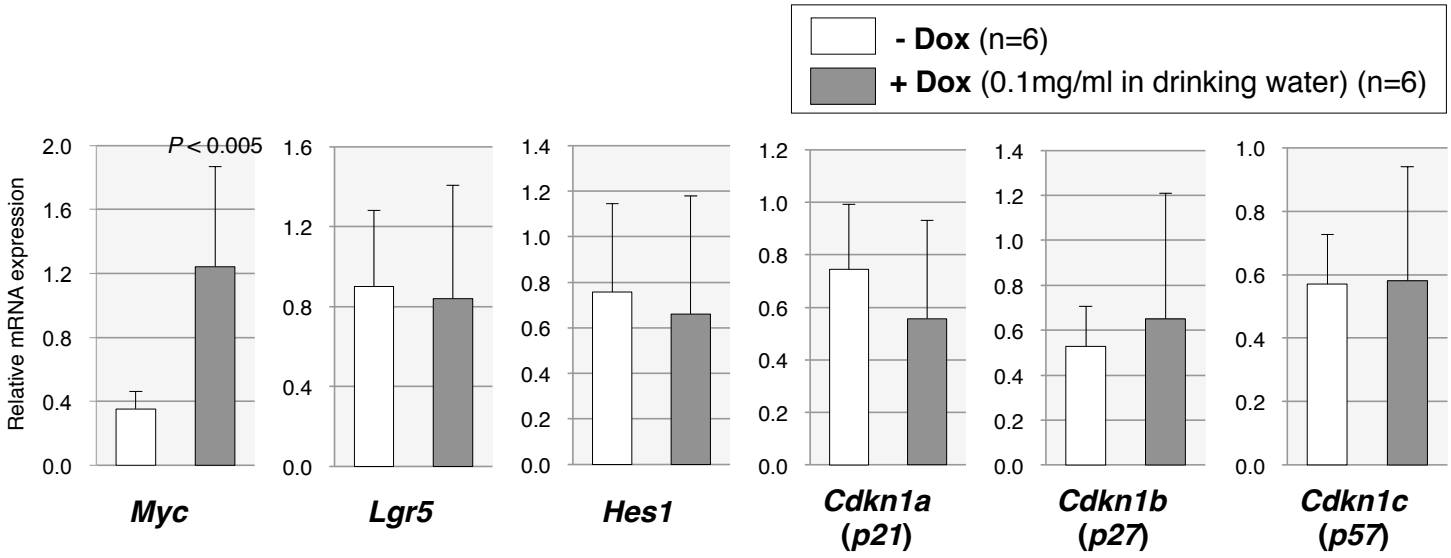

Fig. S9. Lower level of β-catenin induction leads to different patterns of transcriptional activation. qRT-PCR analyses of the Wnt target *Myc*, the ISC marker *Lgr5*, the Notch target *Hes1* and the Cdk inhibitors *Cdkn1a* (*p21*), *Cdkn1b* (*p27*) and *Cdkn1c* (*p57*) in colonic crypts with lower level of β-catenin induction. β-Catenin-inducible mice were treated with 0.1 mg/ml doxycycline in drinking water for 5 days. Although *Myc* is significantly upregulated ($P<0.005$, by Mann–Whitney *U*-test), expression of *Lgr5*, *Hes1* and Cdk inhibitors is not changed. See also Fig. 2B for comparison with the transcription in colonic crypts with higher level of β-catenin induction. Data represent mean ± s.d.

Table S1. Upregulated genes in the colonic crypts with β-catenin induction for 24 hours and 5 days.

Probe ID	Gene symbol	Gene name	Change in expression (fold)	
			24 hours	5 days
14187	BE136769	expressed sequence BE136769	1.0	112.8
14191	Sox4 *	SRY-box containing gene 4	10.2	31.3
14472	H2-Bl	histocompatibility 2, blastocyst	0.7	29.0
14476	Kcnk13	potassium channel, subfamily K, member 13	2.0	21.7
14414	Brwd3	bromodomain and WD repeat domain containing 3	7.8	19.1
14363	Neto2 *	neuropilin (NRP) and tolloid (TLL)-like 2	2.8	18.3
14229	Sp5	trans-acting transcription factor 5	3.8	15.2
14422	LOC625068	Similar to vomeronasal 2, receptor, 2	2.4	13.9
14187	Pnkd	paroxysmal nonkinesiogenic dyskinesia	4.5	13.8
14223	Ascl2 *	achaete-scute complex homolog-like 2 (Drosophila)	2.8	13.6
14242	Susd4	sushi domain containing 4	10.1	12.2
14447	4930550L11	RIKEN cDNA 4930550L11 gene	2.9	11.9
14418	---	Transcribed locus	4.7	10.5
14488	Rpp25	ribonuclease P 25 subunit (human)	7.6	9.5
14188	Foxd1	forkhead box D1	3.4	9.4
14317	2810404F17	RIKEN cDNA 2810404F17 gene	0.9	8.5
14406	---	---	13.0	8.4
14374	Trim12	tripartite motif protein 12	16.6	8.4
14513	Mtap	methylthioadenosine phosphorylase	4.6	8.3
14555	C630043F03	RIKEN cDNA C630043F03 gene	5.2	8.1
14454	Auts2	Autism susceptibility candidate 2	8.8	7.8
14361	Scn2b	sodium channel, voltage-gated, type II, beta	1.9	7.3
14251	Gngt1 *	guanine nucleotide binding protein (G protein), gamma transd	1.8	7.3
14178	Pla2g5	phospholipase A2, group V	1.6	7.2
14447	Diap2	Diaphanous homolog 2 (Drosophila)	10.7	6.9
14482	Hmox1	heme oxygenase (decycling) 1	2.7	6.9
14320	Ascl2 *	achaete-scute complex homolog-like 2 (Drosophila)	3.2	6.8
14422	---	Adult male epididymis cDNA, RIKEN full-length enriched librar	7.8	6.5
14400	6330549D2	RIKEN cDNA 6330549D23 gene	3.0	6.4
14441	Pip5k2b	Phosphatidylinositol-4-phosphate 5-kinase, type II, beta	8.6	6.3
14417	Slc11a2 *	solute carrier family 11 (proton-coupled divalent metal ion tra	24.6	6.2
14489	Tcl1b1	T-cell leukemia/lymphoma 1B, 1	5.3	6.2
14227	Myt1	myelin transcription factor 1	4.7	6.2
14299	2610301F02	RIKEN cDNA 2610301F02 gene	4.0	6.0
14374	Igfbp4 *	insulin-like growth factor binding protein 4	1.4	5.9
14551	Ckb	creatine kinase, brain	0.9	5.9
14411	Clstn2	calsyntenin 2	3.4	5.8
14455	---	---	3.2	5.7
14515	Sgtb	small glutamine-rich tetratricopeptide repeat (TPR)-containin	2.4	5.6
14249	Myc	myelocytomatosis oncogene	2.5	5.5
14356	2310008H0	RIKEN cDNA 2310008H09 gene	4.2	5.4
14517	Nsdhl	NAD(P) dependent steroid dehydrogenase-like	1.8	5.3
14217	Rdh1	retinol dehydrogenase 1 (all trans)	0.8	5.3
14344	C030011O1	RIKEN cDNA C030011O14 gene	3.5	5.2
14385	Vwa2	von Willebrand factor A domain containing 2	1.7	5.0
14264	Slc11a2 *	solute carrier family 11 (proton-coupled divalent metal ion tra	14.9	4.9

14356	Ikbkg *	inhibitor of kappaB kinase gamma	7.6	4.8
14605	Ascl2 *	achaete-scute complex homolog-like 2 (Drosophila)	2.3	4.7
14237	Igfbp4 *	insulin-like growth factor binding protein 4	0.9	4.6
14231	Cfh	complement component factor h	2.9	4.6
14550	Tbc1d9	TBC1 domain family, member 9	2.8	4.6
14486	Arhgdig	Rho GDP dissociation inhibitor (GDI) gamma	1.4	4.5
14196	Ier3	immediate early response 3	2.3	4.5
14277	Acta1	actin, alpha 1, skeletal muscle	3.3	4.4
14509	Lgr5	leucine rich repeat containing G protein coupled receptor 5	1.4	4.3
14228	Hmga2 *	high mobility group AT-hook 2	2.5	4.3
14341	Serhl	serine hydrolase-like	2.1	4.3
14438	---	---	5.4	4.3
14207	5830411J07	RIKEN cDNA 5830411J07 gene	2.7	4.1
14508	Tnni1	troponin I, skeletal, slow 1	6.0	4.1
14188	Phlda1	pleckstrin homology-like domain, family A, member 1	2.1	4.1
14474	D7Wsu130e	DNA segment, Chr 7, Wayne State University 130, expressed	1.2	4.0
14451	C77631	expressed sequence C77631	3.2	4.0
14383	Cnn3 *	Calponin 3, acidic	3.6	4.0
14213	Axin2 *	axin2	1.5	4.0
14382	Mid1	midline 1	7.2	3.9
14401	Prkar1b	protein kinase, cAMP dependent regulatory, type I beta	6.9	3.9
14178	Gcat *	glycine C-acetyltransferase (2-amino-3-ketobutyrate-coenzy	1.4	3.9
14341	A530016O0	RIKEN cDNA A530016O06 gene	4.5	3.9
14219	Epha4	Eph receptor A4	2.3	3.9
14490	Myl7	myosin, light polypeptide 7, regulatory	2.2	3.8
14254	Tgfbr2	transforming growth factor, beta receptor II	3.5	3.8
14510	Ftsj3	FtsJ homolog 3 (E. coli)	2.0	3.8
14323	1700042B14	RIKEN cDNA 1700042B14 gene	3.7	3.8
14432	Mrps14	mitochondrial ribosomal protein S14	5.9	3.7
14536	Fance *	Fanconi anemia, complementation group E	0.7	3.7
14374	Igfbp4 *	insulin-like growth factor binding protein 4	1.3	3.7
14548	Apcdd1	adenomatosis polyposis coli down-regulated 1	3.1	3.7
14248	Trim34	tripartite motif protein 34	6.7	3.7
14370	C030011O1	RIKEN cDNA C030011O14 gene	2.4	3.6
14520	Zfp2 *	zinc finger protein 2	1.9	3.6
14496	Tubb2b *	tubulin, beta 2b	0.9	3.5
14235	Hsp110 *	heat shock protein 110	2.5	3.5
14486	Msx1	homeo box, msh-like 1	1.9	3.5
14224	Defcr4	defensin related cryptdin 4	3.0	3.4
14205	Rac3	RAS-related C3 botulinum substrate 3	1.5	3.4
14572	---	0 day neonate lung cDNA, RIKEN full-length enriched library, c	1.6	3.4
14349	Dmpk	dystrophia myotonica-protein kinase	1.2	3.4
14487	Rbp1	retinol binding protein 1, cellular	0.9	3.4
14471	Elavl1	ELAV (embryonic lethal, abnormal vision, Drosophila)-like 1 (	1.6	3.4
14507	Hmga2 *	high mobility group AT-hook 2	1.6	3.4
14248	Cep68 *	centrosomal protein 68	1.7	3.4
14222	Pfdn5	prefoldin 5	7.8	3.4
14524	Fer1l3	fer-1-like 3, myoferlin (C. elegans)	4.2	3.4
14437	H2-Aa	Histocompatibility 2, class II antigen A, alpha	1.8	3.4
14365	2310008H0	RIKEN cDNA 2310008H09 gene	1.5	3.3
14546	Dctd	dCMP deaminase	1.4	3.3

14234	Mybbp1a *	MYB binding protein (P160) 1a	1.6	3.3
14292	Nap1l1 *	nucleosome assembly protein 1-like 1	1.1	3.3
14465	---	---	3.5	3.3
14416	Iars2	isoleucine-tRNA synthetase 2, mitochondrial	2.6	3.3
14210	Gsta1	glutathione S-transferase, alpha 1 (Ya)	1.5	3.3
14515	Ephb3	Eph receptor B3	1.0	3.3
14557	C130037N1	RIKEN cDNA C130037N17 gene	4.3	3.3
14244	2410005H0	RIKEN cDNA 2410005H09 gene	2.1	3.2
14270	Rnf43	ring finger protein 43	2.6	3.2
14204	Nap1l1 *	nucleosome assembly protein 1-like 1	1.1	3.2
14435	Slc4a1ap	Solute carrier family 4 (anion exchanger), member 1, adaptor p	0.8	3.2
14428	Dgkk	diacylglycerol kinase kappa	5.8	3.2
14493	Sox4 *	SRY-box containing gene 4	1.2	3.2
14390	Mtac2d1 *	membrane targeting (tandem) C2 domain containing 1	3.1	3.2
14478	Vnn1 *	vanin 1	1.9	3.2
14368	Axin2 *	axin2	2.2	3.1
14335	LOC672274	similar to Transcription factor SOX-4	1.2	3.1
14399	Slc30a10 *	solute carrier family 30, member 10	1.7	3.1
14283	2900062L11	RIKEN cDNA 2900062L11 gene	5.0	3.1
14528	Atic	5-aminoimidazole-4-carboxamide ribonucleotide formyltrans	1.0	3.1
14379	Nap1l1 *	nucleosome assembly protein 1-like 1	1.2	3.1
14192	Gas5 *	growth arrest specific 5	1.3	3.1
14186	Egln3	EGL nine homolog 3 (C. elegans)	1.4	3.1
14446	Plaa	phospholipase A2, activating protein	4.3	3.1
14229	Acot1 *	acyl-CoA thioesterase 1	1.1	3.0
14176	Cmkor1	chemokine orphan receptor 1	1.5	3.0
14529	Nol8 *	nucleolar protein 8	1.9	3.0
14564	---	---	3.4	3.0
14486	Enpep	glutamyl aminopeptidase	3.0	3.0
14408	Lrp8	low density lipoprotein receptor-related protein 8, apolipopro	2.5	3.0
14491	Sprr1a	small proline-rich protein 1A	0.8	3.0
14194	Ereg	epiregulin	2.5	3.0
14161	Rbbp9	retinoblastoma binding protein 9	1.5	3.0
14225	Acsl1 *	acyl-CoA synthetase long-chain family member 1	1.2	3.0
14337	C630043F03	RIKEN cDNA C630043F03 gene	1.8	3.0
14534	1110005A0	RIKEN cDNA 1110005A03 gene	1.5	3.0
14547	Phgdh *	3-phosphoglycerate dehydrogenase	1.2	3.0
14313	Smoc2 *	SPARC related modular calcium binding 2	1.2	3.0
14244	Tm4sf5	transmembrane 4 superfamily member 5	2.3	3.0
14158	Hdgf	hepatoma-derived growth factor	1.3	2.9
14436	Sypl	Synaptophysin-like protein	1.8	2.9
14385	1700001G1	RIKEN cDNA 1700001G11 gene	2.0	2.9
14479	2410006H1	RIKEN cDNA 2410006H16 gene	1.2	2.9
14549	Mtm1	X-linked myotubular myopathy gene 1	1.8	2.9
14539	Acpp	acid phosphatase, prostate	0.1	2.9
14237	5630401D2	RIKEN cDNA 5630401D24 gene	1.4	2.9
14554	Kcnj11	potassium inwardly rectifying channel, subfamily J, member 1	1.9	2.9
14267	Cnn3 *	calponin 3, acidic	1.2	2.9
14427	---	Transcribed locus	2.6	2.9
14526	Lrrtm1 *	leucine rich repeat transmembrane neuronal 1	0.9	2.9
14442	---	---	9.8	2.9

14334	Tcf7	transcription factor 7, T-cell specific	2.5	2.9
14321	Ecgf1	endothelial cell growth factor 1 (platelet-derived)	2.3	2.9
14160	Fabp5 *	fatty acid binding protein 5, epidermal	0.7	2.9
14427	---	---	2.0	2.9
14265	Nol5a *	nucleolar protein 5A	1.5	2.9
14514	Umps	uridine monophosphate synthetase	2.6	2.9
14489	Thop1	thimet oligopeptidase 1	1.7	2.9
14402	Agpat7	Nacylglycerol-3-phosphate O-acyltransferase 7 (lysophospha	1.2	2.9
14462	---	0 day neonate thymus cDNA, RIKEN full-length enriched librar	3.1	2.9
14497	---	---	2.7	2.8
14546	Psat1 *	phosphoserine aminotransferase 1	0.7	2.8
14251	Shmt1 *	serine hydroxymethyl transferase 1 (soluble)	1.1	2.8
14164	Tmed6	transmembrane emp24 protein transport domain containing 6	2.4	2.8
14354	C79267	expressed sequence C79267	2.0	2.8
14195	Olr1	oxidized low density lipoprotein (lectin-like) receptor 1	1.2	2.8
14167	Wee1	wee 1 homolog (S. pombe)	1.2	2.8
14567	Snai3	snail homolog 3 (Drosophila)	1.8	2.8
14438	Atp13a3 *	ATPase type 13A3	1.7	2.8
14176	Per2 *	period homolog 2 (Drosophila)	1.6	2.8
14181	Tcfap4	transcription factor AP4	1.2	2.8
14200	Lss	lanosterol synthase	1.3	2.8
14317	Prmt3 *	protein arginine N-methyltransferase 3	1.4	2.8
14264	Jag2	jagged 2	1.0	2.8
14427	1700071K01	RIKEN cDNA 1700071K01 gene	2.1	2.8
14171	B230317C12	RIKEN cDNA B230317C12 gene	2.3	2.8
14220	Mycl1 *	v-myc myelocytomatosis viral oncogene homolog 1, lung carci	1.2	2.7
14288	Nolc1 *	nucleolar and coiled-body phosphoprotein 1	1.6	2.7
14167	Ceacam12	CEA-related cell adhesion molecule 12	1.9	2.7
14342	AA408556	expressed sequence AA408556	1.3	2.7
14555	Cnn3 *	calponin 3, acidic	1.2	2.7
14234	Decr2	2-4-dienoyl-Coenzyme A reductase 2, peroxisomal	0.9	2.7
14225	Id2	inhibitor of DNA binding 2	1.3	2.7
14285	Ppat	phosphoribosyl pyrophosphate amidotransferase	1.6	2.7
14307	Pmm1	phosphomannomutase 1	1.2	2.7
14501	Pla2g2a	phospholipase A2, group IIA (platelets, synovial fluid)	1.1	2.7
14506	Mt4	metallothionein 4	0.9	2.7
14527	Nap1l1 *	nucleosome assembly protein 1-like 1	1.2	2.7
14249	Steap1	six transmembrane epithelial antigen of the prostate 1	1.3	2.7
14509	Nol5	nucleolar protein 5	1.4	2.7
14324	Ube4b	ubiquitination factor E4B, UFD2 homolog (S. cerevisiae)	1.8	2.7
14170	Bid	BH3 interacting domain death agonist	2.6	2.6
14266	Kctd14	potassium channel tetramerisation domain containing 14	4.5	2.6
14526	Tubb2b *	tubulin, beta 2b	1.4	2.6
14364	Whrn	whirlin	1.3	2.6
14457	2310047M1	RIKEN cDNA 2310047M15 gene	2.3	2.6
14402	---	Transcribed locus, weakly similar to XP_417295.1 PREDICTED:	1.1	2.6
14187	Comt	catechol-O-methyltransferase	2.7	2.6
14490	Slc16a3	solute carrier family 16 (monocarboxylic acid transporters), m	1.1	2.6
14174	Tex19	testis expressed gene 19	0.4	2.6
14548	Tmem18	transmembrane protein 18	2.3	2.6
14500	Nolc1 *	nucleolar and coiled-body phosphoprotein 1	1.5	2.6

14510	Psat1 *	phosphoserine aminotransferase 1	0.8	2.6
14267	Prmt3 *	protein arginine N-methyltransferase 3	1.8	2.6
14218	LOC630729	similar to Glutathione reductase, mitochondrial precursor (GR)	1.0	2.6
14486	Dvl2	dishevelled 2, dsh homolog (Drosophila)	0.1	2.6
14573	Amy2	Amylase 2, pancreatic	3.3	2.6
14574	---	Transcribed locus	3.9	2.6
14219	Notch3	Notch gene homolog 3 (Drosophila)	1.7	2.6
14290	1110012J17	RIKEN cDNA 1110012J17 gene	1.2	2.6
14359	B4galnt4	beta-1,4-N-acetyl-galactosaminyl transferase 4	1.0	2.6
14246	Tcof1	Treacher Collins Franceschetti syndrome 1, homolog	1.4	2.6
14387	Slc30a10 *	solute carrier family 30, member 10	1.6	2.6
14312	Mga	MAX gene associated	1.1	2.6
14172	Amacr	alpha-methylacyl-CoA racemase	2.5	2.6
14259	Hsp110 *	heat shock protein 110	2.2	2.6
14374	Pcsk9	proprotein convertase subtilisin/kexin type 9	1.5	2.6
14343	Kpnb1	karyopherin (importin) beta 1	0.8	2.6
14250	E430018J23	RIKEN cDNA E430018J23 gene	2.1	2.5
14167	Nme4	expressed in non-metastatic cells 4, protein	1.3	2.5
14513	Fyttd1	forty-two-three domain containing 1	3.1	2.5
14540	Neto2 *	neuropilin (NRP) and tolloid (TLL)-like 2	0.7	2.5
14292	2310030N0	RIKEN cDNA 2310030N02 gene	1.3	2.5
14377	Apex1 *	apurinic/apyrimidinic endonuclease 1	1.6	2.5
14288	Nolc1 *	nucleolar and coiled-body phosphoprotein 1	2.7	2.5
14350	Sypl	synaptophysin-like protein	1.9	2.5
14302	4933406C10	RIKEN cDNA 4933406C10 gene	1.2	2.5
14211	Jag1	jagged 1	1.5	2.5
14239	2210010N0	RIKEN cDNA 2210010N04 gene	1.4	2.5
14257	Vmd2l1	vitelliform macular dystrophy 2-like protein 1	1.9	2.5
14184	Vnn1 *	vanin 1	1.7	2.5
14539	Htf9c	HpaII tiny fragments locus 9c	1.7	2.5
14324	Npm1	nucleophosmin 1	1.4	2.5
14173	Snrpa1	small nuclear ribonucleoprotein polypeptide A'	1.8	2.5
14478	Vps52	vacuolar protein sorting 52 (yeast)	1.0	2.5
14337	Slc39a10 *	solute carrier family 39 (zinc transporter), member 10	1.2	2.5
14334	Glt25d1	glycosyltransferase 25 domain containing 1	2.1	2.5
14290	Stub1	STIP1 homology and U-Box containing protein 1	1.2	2.5
14399	Rpusd2	RNA pseudouridylate synthase domain containing 2	1.5	2.5
14285	Ccdc3	coiled-coil domain containing 3	1.0	2.5
14235	Npm3	nucleoplasmin 3	1.8	2.4
14183	Nola1	nucleolar protein family A, member 1 (H/ACA small nucleolar	1.8	2.4
14246	Frag1	FGF receptor activating protein 1	1.1	2.4
14508	Arvcf	armadillo repeat gene deleted in velo-cardio-facial syndrome	1.6	2.4
14510	Hars2	histidyl tRNA synthetase 2	1.8	2.4
14487	Dnajc2 *	DnaJ (Hsp40) homolog, subfamily C, member 2	1.4	2.4
14360	Thumpd1	THUMP domain containing 1	1.8	2.4
14213	Prox1	prospero-related homeobox 1	1.8	2.4
14497	AA414993	expressed sequence AA414993	0.2	2.4
14187	Ccl25	chemokine (C-C motif) ligand 25	2.3	2.4
14195	Greb1	gene regulated by estrogen in breast cancer protein	1.5	2.4
14337	Nrip2	nuclear receptor interacting protein 2	1.7	2.4
14350	Polr1e	polymerase (RNA) I polypeptide E	1.7	2.4

14302	4930404H2	RIKEN cDNA 4930404H21 gene	2.6	2.4
14238	Acsl1 *	acyl-CoA synthetase long-chain family member 1	1.1	2.4
14415	Fbxl3	F-box and leucine-rich repeat protein 3	3.1	2.4
14191	Deadc1	deaminase domain containing 1	1.7	2.4
14171	Vav3 *	vav 3 oncogene	0.8	2.4
14237	Ppan	peter pan homolog (Drosophila)	1.9	2.4
14490	Acot1 *	acyl-CoA thioesterase 1	0.9	2.4
14330	6330526H1	RIKEN cDNA 6330526H18 gene	2.4	2.4
14246	D13Wsu177	DNA segment, Chr 13, Wayne State University 177, expressed	1.6	2.4
14550	Nol5a *	nucleolar protein 5A	1.6	2.4
14337	Dach1 *	dachshund 1 (Drosophila)	1.2	2.4
14234	Gsta3	glutathione S-transferase, alpha 3	0.5	2.4
14546	Irf2bp2	interferon regulatory factor 2 binding protein 2	1.4	2.4
14547	Slc38a1	solute carrier family 38, member 1	3.9	2.4
14445	LOC240038	similar to reduced expression 2	0.5	2.4
14177	Thoc4	THO complex 4	1.1	2.4
14528	Cad	carbamoyl-phosphate synthetase 2, aspartate transcarbamyla	1.6	2.4
14260	Rgs16	regulator of G-protein signaling 16	1.3	2.4
14520	Pla2g12a	phospholipase A2, group XIIA	1.1	2.4
14185	Wasf1	WASP family 1	2.0	2.4
14208	Pkia	protein kinase inhibitor, alpha	1.9	2.4
14265	Trp53	transformation related protein 53	1.1	2.4
14521	BC053440	cDNA sequence BC053440	1.4	2.4
14161	Apex1 *	apurinic/apyrimidinic endonuclease 1	1.6	2.4
14563	Cep68 *	centrosomal protein 68	1.6	2.4
14448	---	---	3.8	2.4
14534	2600001A1	RIKEN cDNA 2600001A11 gene	1.1	2.4
14374	Tbx3 *	T-box 3	1.3	2.4
14238	Noc4l	nucleolar complex associated 4 homolog (S. cerevisiae)	2.0	2.4
14556	Alkbh2	alkB, alkylation repair homolog 2 (E. coli)	2.0	2.4
14168	Mut	methylmalonyl-Coenzyme A mutase	0.8	2.4
14353	Kctd15	potassium channel tetramerisation domain containing 15	1.5	2.3
14599	LOC626877	Similar to zinc finger protein 709	3.7	2.3
14504	Ncoa6ip	nuclear receptor coactivator 6 interacting protein	1.4	2.3
14368	Cnn3 *	calponin 3, acidic	1.2	2.3
14296	Lrrc17	leucine rich repeat containing 17	1.1	2.3
14513	Zfyve19	zinc finger, FYVE domain containing 19	0.9	2.3
14220	Cdh8	cadherin 8	4.8	2.3
14220	Mycl1 *	v-myc myelocytomatosis viral oncogene homolog 1, lung carci	1.0	2.3
14566	Mthfd1l	methylenetetrahydrofolate dehydrogenase (NADP+ dependent	1.4	2.3
14486	Wdr12	WD repeat domain 12	1.7	2.3
14376	3321401G0	RIKEN cDNA 3321401G04 gene	1.2	2.3
14221	Shmt1 *	serine hydroxymethyl transferase 1 (soluble)	1.1	2.3
14437	Cyp20a1	cytochrome P450, family 20, subfamily A, polypeptide 1	2.6	2.3
14447	Abtb2	ankyrin repeat and BTB (POZ) domain containing 2	1.6	2.3
14495	Tpm2	tropomyosin 2, beta	0.8	2.3
14176	Per2 *	period homolog 2 (Drosophila)	1.7	2.3
14563	Aldh3b2	aldehyde dehydrogenase 3 family, member B2	1.0	2.3
14606	2410002F23	RIKEN cDNA 2410002F23 gene	1.6	2.3
14217	Efna4	ephrin A4	1.2	2.3
14242	Polr3h	polymerase (RNA) III (DNA directed) polypeptide H	1.5	2.3

14355	2010109N1	RIKEN cDNA 2010109N14 gene	1.4	2.3
14218	Rps18	ribosomal protein S18	1.1	2.3
14560	Apex1 *	apurinic/apyrimidinic endonuclease 1	1.2	2.3
14207	Tex15	testis expressed gene 15	1.1	2.3
14211	Areg	amphiregulin	1.9	2.3
14421	4632427E13	RIKEN cDNA 4632427E13 gene	2.3	2.3
14366	6720401G1	RIKEN cDNA 6720401G13 gene	0.9	2.3
14367	Cnn3 *	calponin 3, acidic	1.1	2.3
14514	Aldoc	aldolase 3, C isoform	1.6	2.3
14588	4732468M1	RIKEN cDNA 4732468M13 gene	0.3	2.3
14541	Ccdc86	coiled-coil domain containing 86	1.5	2.3
14277	Cftr	cystic fibrosis transmembrane conductance regulator homolog	1.0	2.3
14234	Mybbp1a *	MYB binding protein (P160) 1a	1.7	2.3
14476	Rpl24	ribosomal protein L24	1.1	2.3
14186	Ube2h	ubiquitin-conjugating enzyme E2H	0.8	2.3
14557	Picalm	Phosphatidylinositol binding clathrin assembly protein	2.9	2.3
14257	Mtac2d1 *	membrane targeting (tandem) C2 domain containing 1	3.1	2.3
14312	Prdx4	peroxiredoxin 4	0.6	2.3
14336	Snord22 *	small nucleolar RNA, C/D box 22	1.2	2.3
14376	Phgdh *	3-phosphoglycerate dehydrogenase	0.8	2.3
14291	Wdr34	WD repeat domain 34	1.9	2.3
14191	Sox4 *	SRY-box containing gene 4	0.9	2.3
14401	9630027E11	hypothetical protein 9630027E11	0.1	2.3
14239	Krt2-7	keratin complex 2, basic, gene 7	0.9	2.3
14558	2700023E23	RIKEN cDNA 2700023E23 gene	1.5	2.3
14527	Txn2	thioredoxin 2	1.5	2.3
14390	MGC117846	Similar to zinc finger protein 665	1.2	2.3
14380	Rab11fip3	RAB11 family interacting protein 3 (class II)	1.4	2.3
14168	Fgd1	FYVE, RhoGEF and PH domain containing 1	1.8	2.3
14506	Acsl1 *	acyl-CoA synthetase long-chain family member 1	1.1	2.2
14508	Solh	small optic lobes homolog (Drosophila)	2.0	2.2
14384	Nebl	nebulette	1.9	2.2
14524	Cd44	CD44 antigen	1.0	2.2
14486	Cyp2d26	cytochrome P450, family 2, subfamily d, polypeptide 26	3.5	2.2
14596	Snf1lk	SNF1-like kinase	1.7	2.2
14291	8430438M0	RIKEN cDNA 8430438M01 gene	1.6	2.2
14264	Shmt2	serine hydroxymethyl transferase 2 (mitochondrial)	1.0	2.2
14452	BC023969	cDNA sequence BC023969	1.7	2.2
14551	Gloxd1	glyoxalase domain containing 1	2.5	2.2
14157	Ncl *	nucleolin	1.3	2.2
14180	Tfpt *	TCF3 (E2A) fusion partner	1.1	2.2
14206	Dach1 *	dachshund 1 (Drosophila)	1.5	2.2
14301	Reep6	receptor accessory protein 6	1.2	2.2
14159	Sf3b3 *	splicing factor 3b, subunit 3	1.5	2.2
14272	Palld	palladin, cytoskeletal associated protein	2.4	2.2
14184	Pus3	pseudouridine synthase 3	2.4	2.2
14360	Cep68 *	centrosomal protein 68	1.7	2.2
14486	Vav3 *	vav 3 oncogene	0.9	2.2
14456	---	---	1.4	2.2
14266	Phgdh *	3-phosphoglycerate dehydrogenase	0.7	2.2
14556	Rps3	ribosomal protein S3	1.2	2.2

14224	Cdk4 *	cyclin-dependent kinase 4	1.3	2.2
14490	Eef1e1	eukaryotic translation elongation factor 1 epsilon 1	1.9	2.2
14519	Recc1	replication factor C 1	1.1	2.2
14196	1700010I14	RIKEN cDNA 1700010I14 gene	1.5	2.2
14189	Pam	peptidylglycine alpha-amidating monooxygenase	3.8	2.2
14238	2610012O2	RIKEN cDNA 2610012O22 gene	1.9	2.2
14510	Nol11	nucleolar protein 11	0.8	2.2
14577	Zfp192	zinc finger protein 192	0.4	2.2
14527	Prmt1	protein arginine N-methyltransferase 1	1.1	2.2
14242	Ifitm1	interferon induced transmembrane protein 1	0.7	2.2
14335	LOC622534	similar to ribosomal protein L36	1.2	2.2
14171	Vav3 *	vav 3 oncogene	0.8	2.2
14365	1110008H0	RIKEN cDNA 1110008H02 gene	1.4	2.2
14528	Ddx10	DEAD (Asp-Glu-Ala-Asp) box polypeptide 10	1.4	2.2
14231	Gtpbp4 *	GTP binding protein 4	1.3	2.2
14178	Gcat *	glycine C-acetyltransferase (2-amino-3-ketobutyrate-coenzy	1.7	2.2
14163	Fkbp4	FK506 binding protein 4	1.5	2.2
14494	Il12b	interleukin 12b	1.4	2.2
14508	Gtpbp4 *	GTP binding protein 4	1.7	2.2
14346	Gpr22	G protein-coupled receptor 22	1.0	2.2
14252	Gngt1 *	guanine nucleotide binding protein (G protein), gamma transd	0.6	2.2
14418	Seh1l	SEH1-like (S. cerevisiae	1.2	2.2
14287	Bri3bp *	Bri3 binding protein	1.4	2.2
14171	Exosc5	exosome component 5	1.3	2.2
14160	Abce1 *	ATP-binding cassette, sub-family E (OABP), member 1	1.9	2.2
14176	Dnajc2 *	DnaJ (Hsp40) homolog, subfamily C, member 2	1.6	2.2
14279	Rdh9	retinol dehydrogenase 9	1.1	2.2
14511	Idi1	isopentenyl-diphosphate delta isomerase	1.2	2.2
14359	Rps6	ribosomal protein S6	1.8	2.2
14507	Hmga2 *	high mobility group AT-hook 2	1.8	2.2
14441	Odf2	outer dense fiber of sperm tails 2	1.3	2.2
14235	Ptpn5	protein tyrosine phosphatase, non-receptor type 5	4.7	2.2
14275	Utrn *	utrophin	0.9	2.2
14257	Rorc	RAR-related orphan receptor gamma	0.7	2.2
14372	2700081O1	RIKEN cDNA 2700081O15 gene	1.5	2.2
14243	Adhfe1	alcohol dehydrogenase, iron containing, 1	1.3	2.2
14484	2410016O0	RIKEN cDNA 2410016O06 gene	1.7	2.2
14495	Zfr	zinc finger RNA binding protein	1.5	2.2
14236	Cdca4	cell division cycle associated 4	1.5	2.2
14516	Wdr75	WD repeat domain 75	1.7	2.2
14373	F2r	coagulation factor II (thrombin) receptor	0.9	2.2
14512	Ikbkap	inhibitor of kappa light polypeptide enhancer in B-cells, kinas	1.3	2.2
14563	Cnn3 *	calponin 3, acidic	1.2	2.2
14278	Dnttip2	deoxynucleotidyltransferase, terminal, interacting protein 2	1.5	2.2
14480	---	Adult male medulla oblongata cDNA, RIKEN full-length enrich	1.6	2.2
14159	Smoc2 *	SPARC related modular calcium binding 2	1.5	2.2
14533	Xrcc6bp1	XRCC6 binding protein 1	1.6	2.1
14522	Utrn *	utrophin	1.0	2.1
14167	Rcl1	RNA terminal phosphate cyclase-like 1	1.7	2.1
14494	Gas5 *	growth arrest specific 5	1.3	2.1
14561	2600005C20	RIKEN cDNA 2600005C20 gene	1.2	2.1

14486	Ccnd1	cyclin D1	1.7	2.1
14541	Pcgf6	polycomb group ring finger 6	1.5	2.1
14225	Ilf3	interleukin enhancer binding factor 3	0.7	2.1
14592	---	---	1.8	2.1
14350	Utp14a	UTP14, U3 small nucleolar ribonucleoprotein, homolog A (yeas	1.7	2.1
14501	Ikbkg *	inhibitor of kappaB kinase gamma	1.2	2.1
14231	Wdr4	WD repeat domain 4	1.2	2.1
14237	Igfbp4 *	insulin-like growth factor binding protein 4	1.2	2.1
14167	Oprs1	opioid receptor, sigma 1	1.7	2.1
14159	Nup62	nucleoporin 62	1.7	2.1
14517	Hod	homeobox only domain	1.5	2.1
14363	Rora	RAR-related orphan receptor alpha	1.4	2.1
14507	Syncrip *	synaptotagmin binding, cytoplasmic RNA interacting protein	1.2	2.1
14336	Snord22 *	small nucleolar RNA, C/D box 22	1.3	2.1
14283	Ddit4	DNA-damage-inducible transcript 4	1.3	2.1
14499	Zfp2 *	zinc finger protein 2	1.3	2.1
14399	Cyp11a1	cytochrome P450, family 11, subfamily a, polypeptide 1	2.8	2.1
14512	2310061I09	RIKEN cDNA 2310061I09 gene	2.0	2.1
14183	Terf1	telomeric repeat binding factor 1	1.5	2.1
14157	Ncl *	nucleolin	1.5	2.1
14235	Slc1a4 *	solute carrier family 1 (glutamate/neutral amino acid transpor	1.5	2.1
14485	Tead2	TEA domain family member 2	1.1	2.1
14160	Fabp5 *	fatty acid binding protein 5, epidermal	0.7	2.1
14486	Fzd6	frizzled homolog 6 (Drosophila)	1.3	2.1
14210	Agpat1	1-acylglycerol-3-phosphate O-acyltransferase 1 (lysophosph	1.5	2.1
14256	LOC669007	similar to General transcription factor II-I (GTFII-I)	1.4	2.1
14488	Ankrd47	ankyrin repeat domain 47	2.3	2.1
14549	Slc7a1	solute carrier family 7 (cationic amino acid transporter, y+ sys	1.3	2.1
14219	Cbx5	chromobox homolog 5 (Drosophila HP1a)	1.5	2.1
14208	Mrps2	mitochondrial ribosomal protein S2	1.0	2.1
14178	Hsd17b7	hydroxysteroid (17-beta) dehydrogenase 7	1.3	2.1
14383	2810421I24	RIKEN cDNA 2810421I24 gene	0.9	2.1
14302	Wdr77 *	WD repeat domain 77	1.5	2.1
14162	Gart	phosphoribosylglycinamide formyltransferase	1.2	2.1
14491	Polr3g	polymerase (RNA) III (DNA directed) polypeptide G	1.6	2.1
14243	Noc2l	nucleolar complex associated 2 homolog (S. cerevisiae)	1.5	2.1
14439	9230110C19	RIKEN cDNA 9230110C19 gene	1.5	2.1
14289	Nol8 *	nucleolar protein 8	1.2	2.1
14269	---	---	1.1	2.1
14390	Slc39a10 *	solute carrier family 39 (zinc transporter), member 10	1.0	2.1
14182	Lims1	LIM and senescent cell antigen-like domains 1	1.0	2.1
14480	Tbx3 *	T-box 3	1.5	2.1
14160	Ddx18	DEAD (Asp-Glu-Ala-Asp) box polypeptide 18	1.5	2.1
14372	Marcksl1	MARCKS-like 1	1.4	2.1
14410	A430041B07	RIKEN cDNA A430041B07 gene	0.7	2.1
14547	AI173486	expressed sequence AI173486	1.6	2.1
14165	Ctps	cytidine 5'-triphosphate synthase	1.6	2.1
14486	Mvd	mevalonate (diphospho) decarboxylase	1.2	2.1
14482	Ddx21 *	DEAD (Asp-Glu-Ala-Asp) box polypeptide 21	1.4	2.1
14334	Epb4.1l2	erythrocyte protein band 4.1-like 2	1.0	2.1
14287	Bri3bp *	Bri3 binding protein	1.4	2.1

14219	Pfdn2	prefoldin 2	1.3	2.1
14287	Aasdhppt	aminoadipate-semialdehyde dehydrogenase-phosphopanteth	1.5	2.1
14163	Timm8a1	translocase of inner mitochondrial membrane 8 homolog a1 (y	1.4	2.1
14241	Fance *	Fanconi anemia, complementation group E	1.4	2.1
14374	B3galt2	UDP-Gal:betaGlcNAc beta 1,3-galactosyltransferase, polypepti	0.9	2.1
14570	2410127E16	RIKEN cDNA 2410127E16 gene	1.0	2.1
14524	Erdr1	erythroid differentiation regulator 1	2.2	2.1
14510	Ifrd2	interferon-related developmental regulator 2	1.5	2.1
14354	AI464131	expressed sequence AI464131	1.0	2.1
14482	Ddx21 *	DEAD (Asp-Glu-Ala-Asp) box polypeptide 21	1.3	2.1
14530	Wdr5b	WD repeat domain 5B	2.1	2.1
14235	Slc1a4 *	solute carrier family 1 (glutamate/neutral amino acid transpor	1.6	2.1
14539	Ide	insulin degrading enzyme	1.2	2.1
14341	Nfib	nuclear factor I/B	0.8	2.1
14329	5730407O0	RIKEN cDNA 5730407O05 gene	0.3	2.1
14522	Gfer	growth factor, erv1 (S. cerevisiae)-like (augmenter of liver reg	1.4	2.1
14285	2810026P18	RIKEN cDNA 2810026P18 gene	1.4	2.1
14482	C1qbp	complement component 1, q subcomponent binding protein	1.4	2.1
14157	Ncl *	nucleolin	1.2	2.1
14381	---	---	1.4	2.1
14212	Srm	spermidine synthase	1.6	2.1
14520	Hes6	hairy and enhancer of split 6 (Drosophila)	1.7	2.1
14160	AL033314	expressed sequence AL033314	1.0	2.1
14183	Nucb2	nucleobindin 2	1.6	2.1
14407	4833422C13	RIKEN cDNA 4833422C13 gene	0.7	2.1
14483	Stx1a	syntaxin 1A (brain)	1.5	2.1
14283	Wdr43	WD repeat domain 43	1.6	2.1
14489	Pcdhb17	protocadherin beta 17	1.2	2.1
14294	Polr3e	polymerase (RNA) III (DNA directed) polypeptide E	1.6	2.1
14353	Taf4b	TAF4B RNA polymerase II, TATA box binding protein (TBP)-as	1.2	2.1
14248	Gas5 *	growth arrest specific 5	1.6	2.1
14166	Nola2 *	nucleolar protein family A, member 2	1.7	2.1
14166	Nola2 *	nucleolar protein family A, member 2	1.6	2.1
14519	2810453I06	RIKEN cDNA 2810453I06 gene	1.4	2.1
14394	4930403C10	RIKEN cDNA 4930403C10 gene	1.0	2.1
14171	Cstf1	cleavage stimulation factor, 3' pre-RNA, subunit 1	0.3	2.0
14517	Ogt	O-linked N-acetylglucosamine (GlcNAc) transferase (UDP-N-a	1.3	2.0
14550	1500012F01	RIKEN cDNA 1500012F01 gene	1.2	2.0
14559	LOC673503	hypothetical protein LOC673503	1.6	2.0
14266	Tmem34	transmembrane protein 34	1.1	2.0
14552	Cdk6	cyclin-dependent kinase 6	1.5	2.0
14363	Gemin5	gem (nuclear organelle) associated protein 5	0.9	2.0
14182	2610024G1	RIKEN cDNA 2610024G14 gene	1.5	2.0
14176	Drg2	developmentally regulated GTP binding protein 2	1.2	2.0
14558	Lrrtm1 *	leucine rich repeat transmembrane neuronal 1	0.7	2.0
14301	Cd3eap	CD3E antigen, epsilon polypeptide associated protein	1.9	2.0
14521	Eprs	glutamyl-prolyl-tRNA synthetase	1.1	2.0
14286	A930016P21	RIKEN cDNA A930016P21 gene	0.9	2.0
14541	Pwp1	PWP1 homolog (S. cerevisiae)	1.7	2.0
14303	Gusb	glucuronidase, beta	1.2	2.0
14584	Pou6f2	POU domain, class 6, transcription factor 2	2.5	2.0

14484	Gas1	growth arrest specific 1	1.4	2.0
14219	Igfbp4 *	insulin-like growth factor binding protein 4	1.0	2.0
14224	Itga6	integrin alpha 6	0.9	2.0
14337	Slc9a9	solute carrier family 9 (sodium/hydrogen exchanger), isoform	1.2	2.0
14507	Defcr5	defensin related cryptdin 5	1.9	2.0
14439	Mtac2d1 *	membrane targeting (tandem) C2 domain containing 1	4.1	2.0
14524	Metapl1	methionine aminopeptidase-like 1	0.9	2.0
14281	2610019A0	RIKEN cDNA 2610019A05 gene	1.0	2.0
14413	Nkrf	NF-kappaB repressing factor	1.1	2.0
14248	Kcnma1	potassium large conductance calcium-activated channel, subf	1.6	2.0
14207	Art2b	ADP-ribosyltransferase 2b	2.1	2.0
14537	Cpa4	carboxypeptidase A4	1.2	2.0
14270	4933439F18	RIKEN cDNA 4933439F18 gene	0.9	2.0
14245	Nudt6	nudix (nucleoside diphosphate linked moiety X)-type motif 6	1.3	2.0
14369	Grhl3	grainyhead-like 3 (Drosophila)	1.2	2.0
14228	Wdr77 *	WD repeat domain 77	1.6	2.0
14515	Sox9	SRY-box containing gene 9	2.1	2.0
14509	Gtpbp3	GTP binding protein 3	1.4	2.0
14514	Lyplal1	lysophospholipase-like 1	1.6	2.0
14522	Las1l	LAS1-like (S. cerevisiae)	1.6	2.0
14262	Noc3l	nucleolar complex associated 3 homolog (S. cerevisiae)	1.6	2.0
14176	Slc12a2	solute carrier family 12, member 2	1.1	2.0
14339	6720458F09	RIKEN cDNA 6720458F09 gene	0.9	2.0
14549	Nob1	NIN1/RPN12 binding protein 1 homolog (S. cerevisiae)	1.2	2.0
14176	Gtf2f1	general transcription factor IIF, polypeptide 1	1.2	2.0
14379	---	Transcribed locus	1.0	2.0
14204	Hoxa11	homeo box A11	1.0	2.0
14483	Ttc3	tetratricopeptide repeat domain 3	1.8	2.0
14363	2700094K13	RIKEN cDNA 2700094K13 gene	0.8	2.0
14524	Phospho1	phosphatase, orphan 1	1.2	2.0
14235	Hnrpa1	heterogeneous nuclear ribonucleoprotein A1	0.9	2.0
14248	Osbpl10	oxysterol binding protein-like 10	1.2	2.0
14433	2410042D2	RIKEN cDNA 2410042D21 gene	2.3	2.0
14511	2410018C17	RIKEN cDNA 2410018C17 gene	1.8	2.0
14380	BC068171	cDNA sequence BC068171	1.1	2.0
14227	Limd1	LIM domains containing 1	1.1	2.0
14518	Mtac2d1 *	membrane targeting (tandem) C2 domain containing 1	3.3	2.0
14175	Eif4ebp1	eukaryotic translation initiation factor 4E binding protein 1	0.8	2.0
14386	B930041F14	RIKEN cDNA B930041F14 gene	2.9	2.0
14236	Fads1	fatty acid desaturase 1	0.7	2.0
14573	Slc20a2	Solute carrier family 20, member 2	1.1	2.0
14359	Sdhc	succinate dehydrogenase complex, subunit C, integral membra	1.0	2.0
14166	Fbl	fibrillarin	1.3	2.0
14256	Homer1	homer homolog 1 (Drosophila)	2.2	2.0
14246	2610204L23	RIKEN cDNA 2610204L23 gene	1.2	2.0
14357	Gchfr	GTP cyclohydrolase I feedback regulator	1.0	2.0
14508	Serpinh1	serine (or cysteine) peptidase inhibitor, clade H, member 1	1.9	2.0
14250	Ubxd4	UBX domain containing 4	1.0	2.0
14341	D19Bwg135	DNA segment, Chr 19, Brigham & Women's Genetics 1357 expr	1.6	2.0
14158	Uhrf1	ubiquitin-like, containing PHD and RING finger domains, 1	1.3	2.0
14476	Mettl1	methyltransferase-like 1	1.2	2.0

14517	Il1rn	interleukin 1 receptor antagonist	1.1	2.0
14265	Zfp553	zinc finger protein 553	1.4	2.0
14208	Ywhag	3-monooxygenase/tryptophan 5-monooxygenase activation p	1.7	2.0
14169	Rrs1	RRS1 ribosome biogenesis regulator homolog (S. cerevisiae)	1.3	2.0
14336	Surf2	surfeit gene 2	1.4	2.0
14237	Pdk1	pyruvate dehydrogenase kinase, isoenzyme 1	0.5	2.0
14420	Abce1 *	ATP-binding cassette, sub-family E (OABP), member 1	1.9	2.0
14292	Ddah1	dimethylarginine dimethylaminohydrolase 1	1.4	2.0
14234	Bzw2	basic leucine zipper and W2 domains 2	1.0	2.0
14219	Nedd4	neural precursor cell expressed, developmentally down-regult	1.1	2.0
14421	Atp13a3 *	ATPase type 13A3	1.6	2.0
14389	Tfpt *	TCF3 (E2A) fusion partner	1.5	2.0
14389	Ddx31	DEAD/H (Asp-Glu-Ala-Asp/His) box polypeptide 31	2.0	2.0
14301	Ccnd2	cyclin D2	2.2	2.0
14258	Cacna2d1	calcium channel, voltage-dependent, alpha2/delta subunit 1	2.0	2.0
14475	Rpo1-4	RNA polymerase 1-4	1.7	2.0
14224	Cdk4 *	cyclin-dependent kinase 4	1.3	2.0
14586	---	Transcribed locus	1.9	2.0
14372	B230312I18	RIKEN cDNA B230312I18 gene	1.8	2.0
14379	---	---	2.0	2.0
14208	Slc25a30	solute carrier family 25, member 30	1.6	2.0
14523	Hspa1a	heat shock protein 1A	3.7	2.0
14373	Aldh9a1	aldehyde dehydrogenase 9, subfamily A1	1.0	2.0
14603	Acsl1 *	acyl-CoA synthetase long-chain family member 1	1.2	2.0
14266	LOC633640	similar to CG10866-PA	1.7	2.0
14400	BC031748	cDNA sequence BC031748	0.9	2.0
14263	Eif4b	eukaryotic translation initiation factor 4B	1.1	2.0
14495	Supt16h	suppressor of Ty 16 homolog (S. cerevisiae)	0.9	2.0
14254	H2-Ab1	histocompatibility 2, class II antigen A, beta 1	2.5	2.0
14542	2410019A1	RIKEN cDNA 2410019A14 gene	1.7	2.0
14478	2010109N1	RIKEN cDNA 2010109N14 gene	1.4	2.0
14236	6530403A0	RIKEN cDNA 6530403A03 gene	1.3	2.0
14509	Got1	glutamate oxaloacetate transaminase 1, soluble	1.5	2.0
14486	Pole	polymerase (DNA directed), epsilon	1.1	2.0
14498	Timm9	translocase of inner mitochondrial membrane 9 homolog (yea	1.9	2.0
14480	---	---	1.6	2.0
14596	---	---	2.3	2.0
14509	Ppp1r14b	protein phosphatase 1, regulatory (inhibitor) subunit 14B	1.4	2.0
14370	Sox21	SRY-box containing gene 21	1.3	2.0
14363	Trim37	tripartite motif protein 37	1.6	2.0
14511	Sf3b5 *	splicing factor 3b, subunit 5	1.1	2.0
14493	Gpatc4	G patch domain containing 4	1.3	2.0
14227	Syncrip *	synaptotagmin binding, cytoplasmic RNA interacting protein	1.2	2.0
14206	Dnaja3	DnaJ (Hsp40) homolog, subfamily A, member 3	1.1	2.0
14195	Fahd1	fumarylacetoacetate hydrolase domain containing 1	1.2	2.0
14550	Prpf38b	PRP38 pre-mRNA processing factor 38 (yeast) domain contain	0.9	2.0
14222	Msh3	mutS homolog 3 (E. coli)	1.5	2.0
14158	Scd2	stearoyl-Coenzyme A desaturase 2	1.0	2.0
14313	3110005L24	RIKEN cDNA 3110005L24 gene	1.2	2.0
14481	Ppp2r4	protein phosphatase 2A, regulatory subunit B (PR 53)	1.4	2.0
14481	Prps1 *	phosphoribosyl pyrophosphate synthetase 1	1.2	2.0

14209	4933411K20	RIKEN cDNA 4933411K20 gene	2.2	2.0
14521	2600005C20	RIKEN cDNA 2600005C20 gene	1.3	2.0
14190	Brca2	breast cancer 2	1.6	2.0
14266	Pus7	pseudouridylate synthase 7 homolog (S. cerevisiae)	1.2	2.0
14339	Rpl13a	ribosomal protein L13a	1.1	2.0
14412	---	PREDICTED: Mus musculus hypothetical protein LOC626097	1.3	2.0
14158	Impdh2	inosine 5'-phosphate dehydrogenase 2	1.5	2.0
14238	Nsun2	NOL1/NOP2/Sun domain family 2	1.5	2.0
14178	2700038N0	RIKEN cDNA 2700038N03 gene	2.0	2.0
14558	Grwd1	glutamate-rich WD repeat containing 1	1.3	2.0
14481	1110014J01	RIKEN cDNA 1110014J01 gene	1.6	2.0

Genes which were previously identified as Wnt targets in colorectal cancer cell lines (van de Watering et al., 2002; van der Flier et al., 2007) are indicated in grey. A total of 58 probes corresponding to 43 different genes are included in the table. The genes indicated with an asterisk are present more than once in the table.

Table S2. Primer sequences for quantitative real-time RT-PCR

Genes	Forward	Reverse
Actb	5'-CATCCGTAAAGACCTCTATGCCAAC-3'	5'-ATGGAGCCACCGATCCACA-3'
Ascl2	5'-AAGCACACCTTGACTGGTACG-3'	5'-AAGTGGACGTTTGCACCTTCA-3'
Bmi1	5'-ATCCCCACTTAATGTGTGTCCT-3'	5'-CTTGCTGGTCTCCAAGTAACG-3'
Ccna2	5'-AGGCTGACACTCTTTCCGAA-3'	5'-CCTCTGGGGAAAAAGGAAAG-3'
Ccnb1	5'-TGCTTCCTGTTATGCAGCAC-3'	5'-GTGTACAGTTCAGCTGTGCCA-3'
Ccnd1	5'-CATGTATCATCTAGCCATGCACGAG-3'	5'-ATGCACAACAGGCCGCTACA-3'
Cdkn1a	5'-CTGTCTTGCACTCTGGTGTCTGA-3'	5'-CCAATCTGCGCTTGGAGTGA-3'
Cdkn1b	5'-TCGACGCCAGACGTAAACAG-3'	5'-TCTCAGTGCTTATACAGGATGTCCA-3'
Cdkn1c	5'-CGAGGAGCAGGACGAGAATC-3'	5'-GAAGAAGTCGTTCGCATTGGC-3'
Ctnnb1	5'-CCTTGGATATCGCCAGGATGA-3'	5'-CAGATCAGGCAGCCCATCAA-3'
Ephb2	5'-GCCGGCTTTACCTCTTTCGAC-3'	5'-GGCAGGCGAATGTCAAACCT-3'
Ephb3	5'-CATGGACACGAAATGGGTGAC-3'	5'-GCGGATAGGATTCATGGCTTCA-3'
Gpx2	5'-ATGGCTTACATTGCCAAGTCG-3'	5'-TGCCTCTGAACGTATTGAAGTC-3'
Hes1	5'-ATAGCTCCCGGCATTCCAAG-3'	5'-GCGCGGTATTTCCCCAACA-3'
Hopx	5'-ACCAGGTGGAGATCCTGGAGTA-3'	5'-CCAGGCGCTGCTTAAACCAT-3'
Jag1	5'-CCTCGGGTCAGTTTGAGCTG-3'	5'-CCTTGAGGCACACTTTGAAGTA-3'
Jag2	5'-AGTTCCTGGATGGAAGACTGCAA-3'	5'-TGACCAGAGAGCAGGCAAGG-3'
Lgr5	5'-TGCCCCGTGGCTTTCTTATC-3'	5'-TTTCCCAGGCTGCCCATATC-3'
Msi1	5'-CCTCTCACGGCTTATGGGC-3'	5'-CTGTGGCAATCAAGGGACC-3'
Myb	5'-CAATGTCCTCAAAGCCTTTACCG-3'	5'-CATGACCAGAGTTCGAGCTGAGA-3'
Myc	5'-GCTCGCCCAAATCCTGTACCT-3'	5'-TCTCCACAGACACCACATCAATTTC-3'
Notch1	5'-GATGGCCTCAATGGGTACAAG-3'	5'-TCGTTGTTGTTGATGTCACAGT-3'
Notch2	5'-ATGTGGACGAGTGTCTGTTGC-3'	5'-GGAAGCATAGGCACAGTCATC-3'
Pcna	5'-GTCTGCAGATGTGCCCCTTG-3'	5'-GACACGCTGGCATCTCAGGA-3'
Slc12a2	5'-GCCGTACAGACTTCACGAAGATGA-3'	5'-TGTTAGCTGTGCTTGAATGCTCCT-3'
Sox9	5'-GAGCCGGATCTGAAGAGGGA-3'	5'-GCTTGACGTGTGGCTTGTTC-3'